Materials Science-Poland, 42(1), 2024, pp. 62-91
http://www.materialsscience.pwr.wroc.pl/
DOI: 10.2478/msp-2024-0009

Advances in the application of biosynthesized carbon dots as fluorescent probes for bioimaging

Xuechan Li, Jiefang He*

School of Life Science, Guizhou Normal University, Guiyang, Guizhou, China, 550025

Carbon dots (CDs) are emerging as versatile fluorescent nanoprobes for bioimaging applications due to advantages like tunable emissions, excellent biocompatibility, facile surface functionalization, and ease of synthesis. This review summarizes recent advances in applying biosynthesized CDs for sensitive bioimaging. CDs derived from sustainable biomass sources through green techniques like hydrothermal and microwave synthesis demonstrate bright, excitation-tunable photoluminescence spanning visible to near-infrared spectra. Careful control of synthesis parameters and surface passivation strategies enhance quantum yields above 50% comparable to toxic semiconductor dots. Conjugation with polymers, peptides, and recognition elements like antibodies impart solubility and selectivity towards cancer cells and biomarkers. *In vitro* validation in standard lines shows targeted organelle imaging abilities. *In vivo* administration reveals renal clearance pharmacokinetics with preferential tumor accumulation via enhanced permeability effects. Average tumor growth inhibition around 50-80% was achieved in mouse xenografts using CDs-drug formulations through combined therapeutic effects of chemotherapy and photothermal ablation under imaging guidance. However, concerns regarding toxicity from chronic exposures, large-scale reproducible manufacturing, and multimodal imaging capabilities need redressal prior to further clinical translation.

Keywords: *carbon nanodots, hydrothermal synthesis, surface bioconjugation, fluorescence imaging, cancer phototherapy, nanomedicine*

1. Introduction

CDs have emerged as a new class of carbon-based nanomaterials that have attracted tremendous research interest, especially for applications in bioimaging [1]. First discovered accidentally during electrophoretic purification of single-walled carbon nanotubes in 2004, CDs are tiny carbon nanoparticles generally less than 10 nm in size [2]. Compared to traditional semiconductor quantum dots and organic dyes, CDs possess several advantages, such as high aqueous solubility, chemical inertness, resistance to photobleaching, excellent biocompatibility, and tunable photoluminescence [3]. CDs can exhibit a wide range of quantum yields depending on their composition and synthetic conditions. For example, Yang et al. [4] reported a simple hydrothermal method to obtain CDs, but with a poor quantum yield of 1.3%. Typical QY values span from single digits for pristine CDs up to 20% for well-optimized formulations with extensive surface passivation. These properties make them highly suited as fluorescence probes for a variety of *in vitro* and *in vivo* bioimaging studies, including cellular labeling, targeted organelle imaging, tumor diagnosis, drug delivery tracking, and more [5, 6].

CDs can be synthesized via two main approaches—a top-down method involving breaking apart bulk carbon structures and bottom-up routes that build them up from molecular precursors [7]. While physical techniques like laser ablation [8], arc discharge [9] and electrochemical oxidation [10] were initially used, the focus has now shifted more towards wet chemical methods, which offer better control over properties. Of particular interest is the biosynthesis of CDs from natural, biomass-derived precursors, which provides additional advantages of sustainability, biocompatibility, and abundance of surface functional groups for further modification [11]. Various biological sources ranging from milk, egg, honey, and fruit extracts

* E-mail: v15513880913@163.com

to plant leaves, fruit peels, and algal extracts have been utilized as starting materials [12]. Key techniques for CD biosynthesis include one-step heating by hydrothermal treatment or microwave irradiation, ultrasonic and enzymatic synthesis routes [13]. Careful control of synthetic parameters allows tuning the size, surface chemistry, and photoluminescence properties of biosynthesized CDs for tailored bioimaging applications [14].

The bright multicolor photoluminescence of CDs is one of their most important optical signatures that has received great research attention. While the definitive mechanisms behind their excitation-dependent emissions are still under debate, it likely arises from a combination of quantum confinement effects, zigzag sites, various emissive traps and surface defects [15, 16]. By modulating synthetic conditions, CDs exhibiting fluorescence across the visible spectrum and into the near-infrared (NIR) region can be obtained. Biosynthesized CDs, in some cases, have quantum yields comparable to or exceeding traditional semiconductor quantum dots [17]. Surface passivation with organic ligands and polymers during or after synthesis has been important to enhance their fluorescence brightness [18]. In addition, CDs also demonstrate excellent photostability and large two-photon absorption cross sections for deeper tissue imaging [19].

The surface chemistry and availability of functional groups play a vital role in determining CDs' properties and their interactions in the biological environment [20]. Pristine biosynthesized CDs may have high hydrophilicity but limited colloidal stability and biofunctionality [21]. Surface modification with polymers like polyethylene glycol (PEG) and biological macromolecules has been important to impart solubility and biocompatibility [22]. In addition, functionalization with targeting ligands extends their application for selective recognition of receptors overexpressed on cancer cells [23]. Conjugation to therapeutic agents transforms fluorescent CDs into multifunctional theranostic probes. The rich surface chemistry of biosynthesized CDs thus offers flexibility for further tuning and bioconjugation for sensitive bioimaging and biosensing.

In addition to their attractive optical properties, the nanoscale dimensions of biosynthesized CDs also play a crucial role in governing their interactions with biological systems at the molecular level. The high surface-area-to-volume ratio and abundant surface functional groups of these quantum-sized particles facilitate their dynamic engagement with proteins, nucleic acids, lipid membranes, and other nanoscale components that make up the complex cellular machinery [24, 25]. Hydrophobic, electrostatic, and hydrogen bonding forces drive the spontaneous assembly of CDs with these biomolecular interfaces to modulate cellular uptake and intracellular trafficking as well as downstream biological responses in the intricate physiological environment [26]. Probing the nature and mechanisms of such nano-bio interactions is therefore vital to understanding CD behavior *in vitro* and *in vivo* for tailoring designs towards desired bioimaging outcomes while mitigating unintended toxicities [27, 28].

Due to a combination of desirable properties like bright multicolor emissions, excellent biocompatibility, surface tailorability, and ease of synthesis, biosynthesized CDs have shown immense application potential as fluorescent nanoprobes. Their implementation for specific *in vitro* and *in vivo* bioimaging applications is the focus of this comprehensive review. Key aspects ranging from favored biosynthesis routes, extensive optical characterization, surface bioconjugation strategies, and demonstration of sensitive bioimaging in diverse biological systems will be covered. Both fundamental photophysical analysis of emissions and practical bioanalytical applications are discussed to provide a holistic picture of the latest advancements with biosynthesized CDs as fluorescent probes for bioimaging.

2. Methods for biosynthesis of CDs

2.1. Top-down vs bottom-up approaches

CDs can be synthesized via two broad approaches: top-down methods that break down carbon structures into nanosized dots and bottom-up methods that build them up from molecular

precursors. Early synthesis of CDs was dominated by top-down techniques, including arc discharge, laser ablation, and electrochemical oxidation. For instance, Raniszewski et al. [29] prepared fluorescent CDs of around 3–5 nm diameter by arc discharging graphite. The coarse carbon soot formed was then oxidized with nitric acid to give water-soluble luminescent nanoparticles. Laser ablation has also been implemented by irradiating graphite or carbon nanopowder suspended in liquids with pulsed laser beams, fracturing them into CDs of 3–10 nm size [30]. Electrochemical approaches (Fig. 1A) rely on anodic oxidation of carbon electrodes in electrolyte solutions, which generate carbonaceous species that nucleate into CDs [31, 32]. However, such physical techniques offer little control over properties or yield.

In contrast, bottom-up wet chemical methods via molecular assembly of small precursors have become more popular as they allow better regulation of CD size and optical properties. Hydrothermal treatment (Fig. 1B) is one of the most facile and economical methods—direct heating of precursors like citric acid or plant extracts in water generates emissive CDs within a few hours [33, 34]. Microwave-assisted heating (Fig. 1C) can produce CDs even faster by rapid decomposition of precursors [35]. Ultrasonication has also been implemented to break down carbon-rich starting materials. Such bottom-up assembly-based growth allows tuning particle size and surface chemistry to desired specifications. It also enables the use of biomass-derived precursors for simple and sustainable biosynthesis compared to top-down bulk disintegration techniques.

Therefore, while physical top-down techniques marked the first reports on CD synthesis, more recent work has focused extensively on bottom-up assembly of molecular precursors as it offers unparalleled flexibility in materials design. Environmentally benign synthesis routes utilizing plant extracts or waste biomass as starting materials add further value for scalability. Careful optimization of these bottom-up techniques also facilitates excellent control of properties like size, surface chemistry, and fluorescence emissions, which can be tailored to the needs of bioimaging and other applications.

Table 1. Common source for CDs synthesis

Source	Ref.	Source	Ref.
Spinach	(39,136–139)	Onion	(40,140–143)
Apple	(41,144,145)	Orange	(42,146,147)
Trapa bispinosa	(148)	*Cannabis sativa*	(149)
Neem	(43,150)	Cocoons	(44,151)
Coffee	(45,152–154)	Oils	(46,155,156)
Milk	(47,157,158)	Egg white	(48,159,160)
Honey	(49,161,162)	Yeast extract	(163)

2.2. Common precursors: biomass sources and the advantages of biosynthetic routes

The choice of precursors is crucial as it defines components and surface chemistry of as-obtained CDs to a large extent. Many carbon-rich small molecules have been utilized, with citric acid being the most common due to its carbon scaffold and abundance of carboxyl groups for surface passivation [36]. Other organic acids like tartaric acid [37] and amino acids [38] have also yielded fluorescent CDs. Plant extracts provide a direct one-step biosynthetic route utilizing the rich bioactive components (Table 1) – leaves, fruits, peels and stem extracts from sources like spinach [39], onion [40], apple [41], orange [42], and neem [43] have been implemented. Waste biomass like silk cocoons [44], coffee grounds [45], and waste frying oils [46] offer sustainable precursors while milk [47], egg white [48], and honey [49] exemplify bioderived materials for simple synthesis.

More recently, algal extracts from *Chlorella* [50], *Sargassum* [51], and other genera [52, 53] have been explored for facile biosynthesis of CDs. Algae cultivation does not compete for arable land and utilizes unwanted CO_2, providing environmental and ethical advantages. Many algae are also rich in antioxidants, vitamins, and other health-promoting components, which translate into beneficial surface functionalization. Advanced material extraction without sacrifice makes algal biomass an exciting renewable precursor. Agnol et al. [54] prepared bright green fluorescent CDs in a

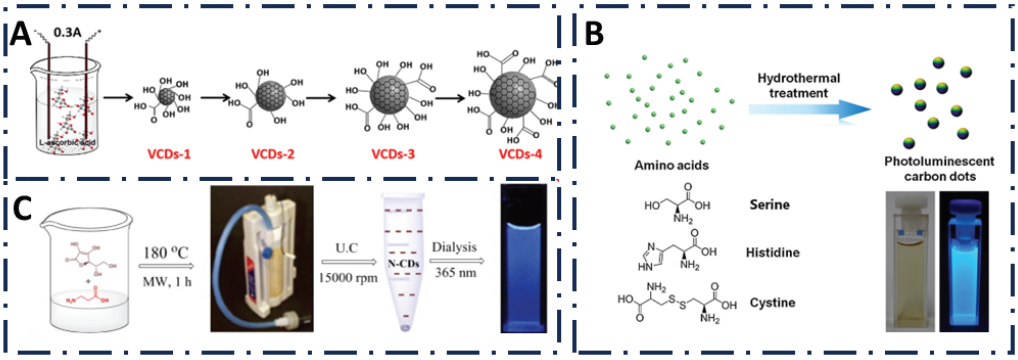

Fig. 1. (A) Fabrication of CDs by a one-step electrochemical oxidation method [32]; (B) Preparation procedure of CDs by hydrothermal treatment of amino acids [34]; (C) Microwave-assisted green synthesis of N-doped carbon dots [35]

single step by hydrothermal treatment of commercially procured Spirulina powder. The protein-rich microalgal extract likely provided both scaffolding and capping agents. In another report, nitrogen and sulfur-doped CDs were synthesized using *Dunaliella salina* macroalgal biomass as a precursor [55]. Advantageously, compared to synthesis with other biomass sources, the yield of CDs from this seaweed source was found to be exceptionally high.

While a wide range of carbon-rich precursors have been utilized, building CDs from waste or naturally derived biomaterials confers them biocompatibility, sustainability, and potential biological functionality. Abundant surface groups also aid water dispersibility and defer agglomeration compared to graphene or carbon nanotubes. Environmentally sound biomass precursors coupled with facile synthesis provide a convenient biosynthetic toolbox for generating CDs [11]. Algal sources, in particular, offer renewed biomaterials advantage. Bottom-up assembly harnessed with such bioderived, value-added components allows the design of bespoke bright fluorescent CDs in an economical and eco-friendly manner.

2.3. Key synthesis techniques: hydrothermal, microwave-assisted, and ultrasonication

While a diversity of precursors have been utilized, the synthesis technique plays an equally crucial role in directing the formation of CDs with desired optical properties. Hydrothermal treatment is one of the most common and versatile methods for CD biosynthesis. Direct heating of precursor solutions in sealed autoclave vessels at high temperatures (100–220°C) and autogenous pressures creates favorable conditions for dehydration, polymerization, and carbonization reactions to occur [56]. The harsh solvothermal environment provides energy for bond breakage and reformation – small molecules assemble into larger carbon scaffolds, which crystallize into CDs a few nanometers wide [57]. Zhang et al. [58] synthesized six types of nitrogen-doped CDs (NCDs) at different hydrothermal temperatures from 120°C to 220°C using citric acid and ammonia solution. Results showed that as temperature increased, carbonization degree and carbon/oxygen ratio increased while functional groups, nitrogen doping level, and fluorescence lifetime remained similar (Fig. 2A). The quantum yield, UV-vis absorbance, and photoluminescence intensity of the NCDs initially increased from 120°C to 180°C and then decreased at higher temperatures with a maximum of 35.4% at 180°C.

Microwave-assisted synthesis works on similar principles but offers a faster response as polar precursor molecules rapidly heat up under microwave irradiation. Dielectric heating induced by an alternating electric field causes molecular friction and decomposition [59]. As temperature

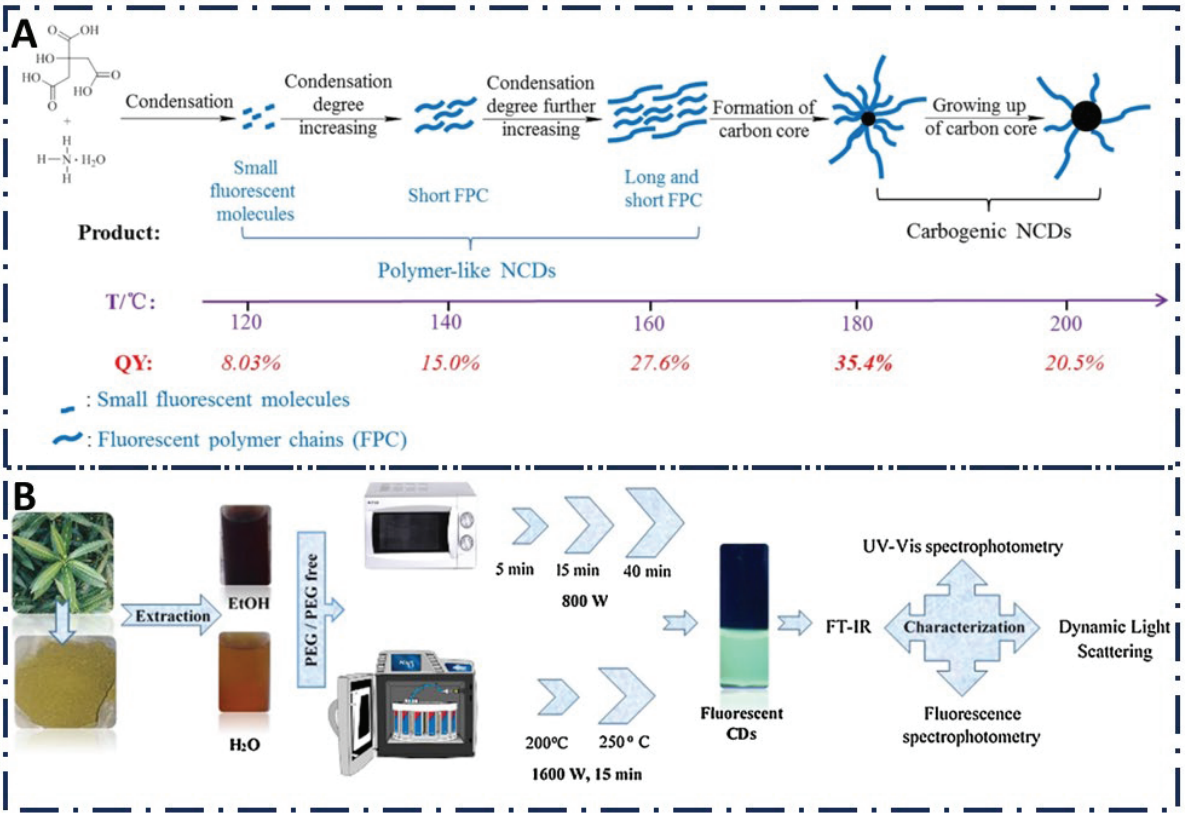

Fig. 2. (A) NCDs prepared using hydrothermal method with different temperature with different QY [58]; (B) MWO and MAH synthesis of CDs from Nerium oleander leaf extracts [61]

rises exponentially, it creates high pressures in sealed reaction vials, leading to CD nucleation. The whole process finishes within minutes. For example, palm kernel shell biomass waste was used as a precursor to synthesize CDs via a microwave irradiation method [60]. CDs were successfully produced with sizes of 6-7 nm in diameter. All CDs contained hydroxyl and alkene functional groups from the transformation of the palm kernel shell. Simsek et al. [61] synthesized fluorescent CDs from *Nerium oleander* leaf extracts using two microwave-based methods—a domestic microwave oven (MWO) and a microwave-assisted hydrothermal (MAH) synthesizer (Fig. 2B). They investigated how factors like extract type, reaction time, temperature, and adding a surface passivation agent (polyethylene glycol) affected CD properties like particle size, surface charge, and photoluminescence intensity. The results showed that MWO synthesis for 40 minutes with an added passivation agent gave CDs a ten times higher fluorescence compared to shorter reaction times. MAH synthesis at 250°C gave the highest photoluminescence intensity. Adding a passivation agent dramatically decreased particle size from 288–825 nm to 2.6–5.7 nm for MAH synthesis. For MAH synthesis, the increasing temperature made the CD surface charge less negative. The extract type affected particle size and surface charge depending on the solvent used. Overall, MWO gave better photoluminescence enhancement compared to MAH, which allowed synthesis in shorter times. Faster kinetics favor the formation of smaller particles with better quantum confinement. Microwave heating also consumes much less energy, making it attractive for scalable manufacturing.

Sonication techniques use powerful ultrasonic waves to create acoustic cavitation, which provides the energy for precursor decomposition and CD assembly. By avoiding harsh heating conditions,

sonochemical methods provide more control over the growth process [62]. However, extended reaction durations of two hours to even 96 hours are usually required to produce brightly emissive CDs. The technique has shown promise for scaling up due to its easier processing. Autoclave-free sonication-enabled synthesis also ensures safety.

In summary, hydrothermal and microwave-based methods have been the most widely adopted as facile, energy-efficient tools for rapid biosynthesis of fluorescent CDs. Sonication approaches offer moderate alternatives avoiding harsh temperatures or pressures. The technique employed plays a definitive role in all stages of precursor transformation - breakage, nucleus formation, growth, and termination of CDs. Fine-tuning of synthesis parameters hence allows customization of optical properties for intended bioimaging and sensing applications.

3. Optical Properties of Biosynthesized CDs

3.1. Tunable photoluminescence and excitation-dependent emissions

The bright photoluminescence of CDs spanning the visible and near-infrared (NIR) spectrum is their defining signature that has greatly enabled bioimaging applications. Understanding and controlling the optical properties is, hence, key to further unlocking their analytical and biomedical potential. CD emissions tend to be broadly tunable and excitation wavelength dependent, which offers opportunities but also poses challenges regarding mechanistic interpretations.

By rationally choosing precursors and judiciously controlling synthesis parameters, emissions can be tuned spanning blue, green, yellow, orange, and red spectral windows [63]. Extending photoluminescence (PL) into the red and NIR regions has been important to minimize background interference from autofluorescence of biological samples for more sensitive bioimaging [64]. The use of sulfur and nitrogen-rich precursors generally allows the obtaining of long wavelength emissive CDs. For instance, Li et al. [39] developed a method to synthesize NIR fluorescent CDs (R-CDs) from spinach via a one-step solvothermal treatment. The R-CDs exhibited maximum fluorescence emission at 680 nm, high quantum yield of 15.34%, excellent water solubility, remarkable photostability, negligible toxicity, and superior bioimaging capability. Jiang et al. [65] synthesized a new type of CD (N-CDs-F) by doping nitrogen and fluorine using ammonium fluoride during a solvothermal process. The resulting N-CDs-F had a donor-π-acceptor structure, which gave them unique optical properties. Compared to undoped carbon dots, the N-CDs-F exhibited broad UV-vis-NIR absorption from 250–1050 nm and efficient excitation upconversion fluorescence under two-, three-, and four-photon laser excitation up to 2000 nm. The QY of the N-CDs-F and the undoped CDs at λex/λem of 710/772 nm are calculated to be 9.8% and 8.1%, respectively. The N-CDs-F also showed larger multiphoton absorption cross sections, with the three-photon cross section over two times greater than previous organic compounds. Analysis suggested the special chemical structure of N-CDs-F, facilitated by extensive hydrogen bonding networks, enabled delocalized conjugated systems that lowered the HOMO-LUMO gap and enhanced nonlinear optical behavior. Such careful modulation of synthesis conditions hence allows the development of application-specific fluorescent CDs. Similar performance has also been observed by many biosynthesized CDs (Fig. 3) [66, 67].

In addition to tunable emissions under a single excitation wavelength, CDs also demonstrate prominent excitation-dependent behavior where the emitted PL peak progressively red shifts with increasing excitation wavelength. This optic signature has been observed across CDs derived from sources as diverse as lemon juice [68], Aegle Marmelos [69], spices [70], and *Azadirachta indica* [71]. While excitation-dependent emissions can be a practical way to obtain multicolor readouts from biocompatible nanoprobes on a single testing platform, the mechanism behind this phenomenon still remains ambiguous and under debate. Explanations invoke varying emissive sites, a distribution of particle sizes, as well as diverse surface defects and functional groups, resulting in a manifold of

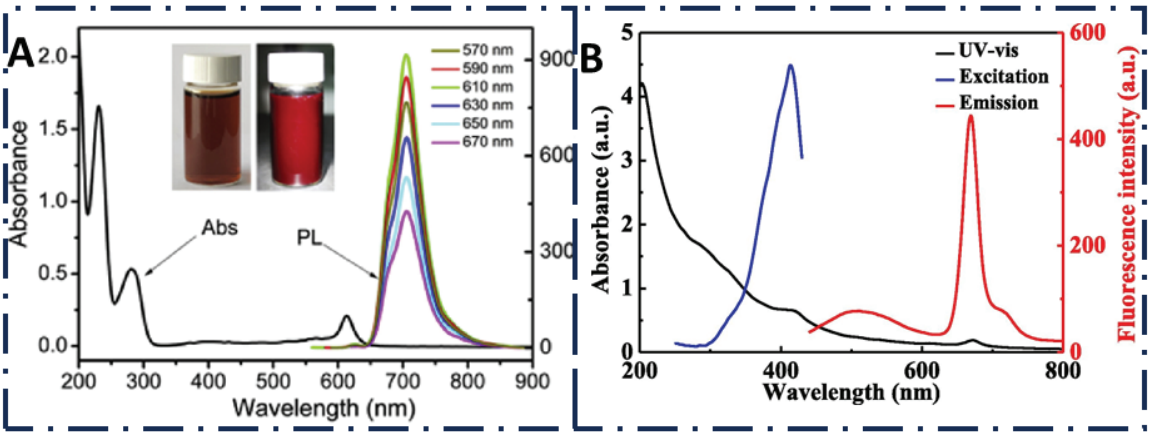

Fig. 3. UV–visible absorption spectrum and PL emission spectra of the (A) NIR-CDs derived from lemon juice [66] and (B) dual-emission CDs derived from black pepper [67]

energy levels that lead to versatile recombinations under assorted excitation energies [72]. Further research using advanced spectroscopic techniques and theoretical simulations is still needed to completely resolve the structure-property-function relationships.

In summary, facile tunability of emissions across the visible spectrum, access to NIR region to avoid background interference, and signature excitation-dependent behavior leading to myriad color readouts offer both opportunities as well as riddles regarding biosynthesized CDs as fluorescent bioprobes. Rational optimization of all these dimensions can vastly expand their applicability for sensitive quantification, multiplexed assays, and multimodal imaging of complex biological phenomena.

3.2. Effects of synthetic conditions and surface passivation on optical properties

While CDs can demonstrate excitation-tunable emissions spanning the visible spectrum, careful optimization of synthesis parameters allows the direction of desired optical outputs tailored to imaging needs. Furthermore, the as-obtained, crude CDs have inferior quantum yields that can be enhanced via surface engineering with ligands and polymers. Such surface passivation impacts not only brightness but also spectral distribution of emitted photons.

Harsh hydrothermal syntheses generally result in greater carbonization and more surface defects, which impact optical signatures. For instance, Han et al. [73] systematically analyzed the effects of hydrothermal reaction temperature on the photoluminescence properties of CDs. They found that a reaction temperature of 200°C was optimal for synthesizing CDs with strong fluorescence. The CDs prepared at 200°C exhibited an emission peak at 414 nm when excited at 340 nm and a quantum yield of about 22% (Fig. 4A). This finding is consistent with the results reported by Li et al., [74] who also investigated the influence of hydrothermal reaction temperature on CD properties. Their work further confirmed that 200°C is a critical threshold for optimizing CD fluorescence. They observed that increasing the reaction temperature from 170°C to 200°C enhanced the fluorescence intensity of the CDs (Fig. 4B). However, temperatures exceeding 200°C led to a significant decrease in fluorescence. Li et al. provided additional insights into the underlying mechanisms. They proposed that temperatures below 200°C are insufficient for effective CD core formation and surface defect reduction. In contrast, temperatures above 200°C cause excessive carbonization, destroying the surface fluorophores and quenching the emission. Furthermore, their work revealed that

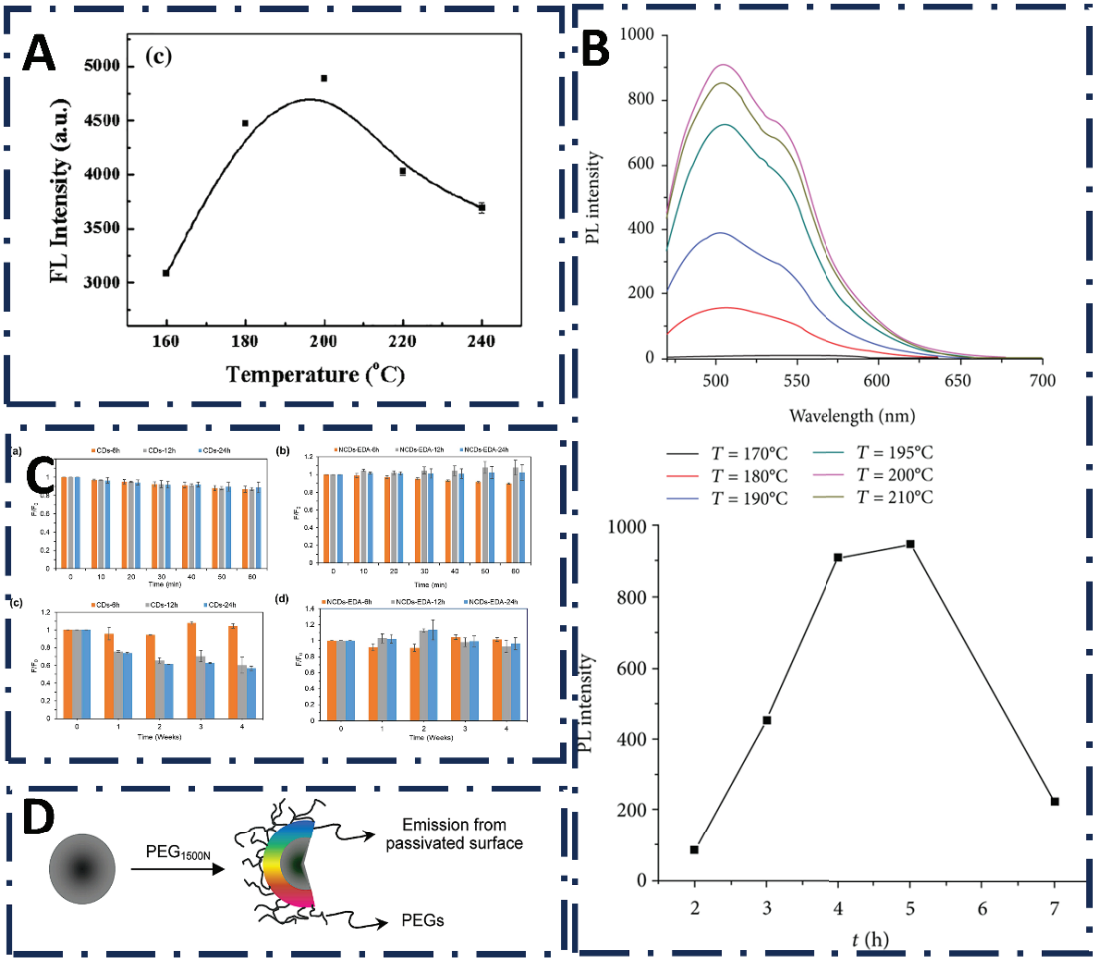

Fig. 4. (A) The effect of reaction temperature on the synthesis of CDs [73]; (B) Effect of reaction temperatures and reaction times on the PL spectra of CDs [74]; (C) The relative fluorescence intensity (F/F_0) of CDs and NCDs-EDA (1.0 mg/mL) under (a, b) UV illumination (365 nm), (c, d) visible light [76]; (D) Covalent passivation of CDs with PEG1500N [77]

the reaction temperature also impacts the nitrogen doping level in CDs, with higher temperatures promoting more effective decomposition of nitrogen precursors.

Apart from synthesis parameters, surface functionalization of as-prepared crude CDs has proven pivotal for amplifying fluorescence brightness. Diverse surface passivating agents have been implemented, spanning small ligands, crosslinkers, macromolecular coatings, and thin-layered shells [75]. Amino acids like cysteine and organic species with multiple amine or thiol moieties interact via electrostatic attractions or covalent linkages with abundant carboxyl and hydroxyl groups on biosynthesized CDs to null surface dangling bonds. For instance, Watcharamongkol et al. [76] used ethylenediamine (EDA) as a nitrogen doping agent to synthesize NCDs via a hydrothermal method from cassava pulps. EDA was used together with cassava pulp to prepare NCDs and introduce nitrogen functional groups into the carbon dots. With this nitrogen doping it was possible to improve the optical and chemical properties of the CDs. NCDs synthesized with EDA (NCDs-EDA) exhibited five times higher fluorescence intensity compared to undoped carbon dots under 360 nm

excitation. NCDs-EDA also showed higher fluorescence quantum yield (36.9%) than undoped CDs (6.6%) synthesized under the same conditions. NCDs-EDA demonstrated higher photostability under UV illumination and visible light compared to undoped CDs (Fig. 4C). Polymer coatings like PEG and oligochitosans also similarly curtail non-radiative relaxations. An interesting review by Peng et al. [22] concluded that PEG has been widely used to passivate CDs, enhancing properties like fluorescence intensity. For example, one study showed that amine-terminated PEG1500 greatly increased the brightness of C-dots made from laser-ablated graphite (Fig. 4D) (77). PEG has also been explored as a solvent, matrix, or carbon source for making CDs. The authors discussed how the molecular weight and structure of PEG impact properties like C-dot size and emission wavelength. Smaller PEG chains tend to produce smaller, blue-emitting C-dots. The proposed mechanism involves PEG chains breaking down and aggregating into aromatic, electron-rich cores surrounded by oxygen-rich hydrophilic surfaces. Therefore, engineering the interfacial layer around the light-emitting CD core directly amplifies brightness to levels comparable with toxic semiconductor quantum dots.

3.3. Chiroptical properties of biosynthesized CDs

Many biomass precursors used for CD synthesis, such as plant extracts, amino acids, and proteins, are inherently chiral in nature. The asymmetric arrangement of surface functional groups or the incorporation of chiral biomolecules during hydrothermal carbonization can result in CDs with chiral surfaces [78]. This chirality can be probed through techniques like circular dichroism spectroscopy and circularly polarized luminescence (CPL) [79].

Zhang et al. [80] developed CDs-composited G-quartet hydrogels capable of emitting CPL. Utilizing a novel one-step microwave-assisted synthesis, this research not only simplified the fabrication process but also introduced a method to control the chirality and CPL properties of the hydrogels through the addition of metal ions, particularly potassium ions. The composite hydrogels demonstrated exceptional CPL performance, with a dissymmetry factor (g_lum) reaching up to 10^{-1}, markedly surpassing most existing CPL materials in terms of efficiency. This remarkable achievement indicates a significant leap forward in the development of CPL materials, offering potential applications in anti-counterfeiting and information encryption technologies. The study further explored the influence of K^+ ions on the helical structure of the hydrogels, achieving reversible control between left-handed and right-handed configurations. These examples demonstrate that the synthetic methods described in our work, particularly hydrothermal treatment and microwave-assisted synthesis, can preserve the chiral nature of biomass precursors and translate it to the resulting CDs. However, the extent of chirality transfer and its impact on CD properties likely depends on factors such as precursor type, reaction conditions, and post-synthesis modifications.

4. Surface Functionalization and Bioconjugation

4.1. Importance of surface chemistry for solubility and biocompatibility

While the carbon core imparts characteristic photoluminescence, the surface chemistry and availability of functional groups on CDs play a pivotal role in governing their interactions and compatibility in biological systems. The surface state also determines lifetime via colloidal stability in aqueous dispersions. Further bioconjugation for sensitive bioimaging hinges on tailoring the interfacial layer appropriately.

Pristine CDs synthesized from biomolecules and waste sources using green techniques may offer sustainability but lack long-term stability due to irreversible aggregation arising out of interparticle hydrophobic interactions and π-π stacking. Surface oxidation techniques, as well as response reactions with amines, thiols, and carboxylic acids, help imprint hydrophilic groups like hydroxyls [81]

and carboxyl [82] as well as amides and amines [83] to promote water dispersibility. Amphiphilic polymers like oligochitosans [84] and PEGylated lipids [85] can also be grafted to produce stable glycoprotein-like nanoparticulates. The introduction of zwitterionic moieties or the construction of hydration layers prevents opsonization and unwanted biofouling for prolonged shelf life.

In addition, surface passivation is also mandated to mitigate the potential cytotoxicity of nascent CD formulations. While toxicity is generally lower compared to graphene and CNTs due to lack of sharp edges, factors like dose, dimensions, and surface groups do play a role. Conversion of reactive groups and enrichment with biocompatible ligands hence enhances bioresponse. For instance, Havrdova et al. [86] found the surface functionalization and resulting surface charge of CDs greatly affect their toxicity profile (Fig. 5). Pristine CDs with a negative charge from carboxylic groups (CDs-Pri) showed a stimulatory effect on cell proliferation at low doses of 5–50 μg/mL. However, at higher doses, they induced G2/M cell cycle arrest, caused higher oxidative stress and reactive oxygen species (ROS) production compared to other CDs, and altered cell morphology. Despite this, they did not enter the cell nucleus. CDs-Pri had an IC50 value of 300 μg/mL. In contrast, PEG-modified CDs with a neutral charge (CDs-PEG) did not affect cell morphology, cell cycle progression, or ROS levels even at high doses. They were the most biocompatible CDs and also did not enter the cell nucleus. Their toxicity (IC50) was similar to CDs-Pri at 300 μg/mL. Positively charged PEI-modified CDs (CDs-PEI) exhibited the highest toxicity of the three CDs, with the lowest IC50 of around 50 μg/mL. CDs-PEI entered the cell nucleus, caused significant morphological changes, induced G0/G1 cell cycle arrest, and stimulated considerable oxidative stress. Likewise, oligochitosan coating of peanut-derived dots was important for biocompatible imaging applications, as reported by Ma et al. [87] Therefore, rational surface passivation through oligomer grafting and polymer entrapment integrates colloidal stability and biological stealth for wider imaging adoption.

4.2. Strategies for functionalization: polymers, biomolecules, and surface ligands

While pristine CDs offer tunable fluorescence, their bioimaging sensitivity and selectivity are enhanced manifold through surface functionalization with recognition elements for the molecular targets. Common functionalization strategies rely on coating CDs with polymers, biomolecular ligand attachment, and integration of stimuli-responsive small molecule groups that render them "smart."

Among polymeric coatings, oligo-peptides [88], proteins like BSA [89], as well as charged species like chitosan [90] and polyethyleneimine [91] have been extensively implemented to boost water solubility. Hydrophilic polymers like PEG provide extensive steric stability and modify pharmacokinetics by reducing renal clearance and increasing circulation half-life. Gonçalves and Silva [92] used PEG200 to functionalize CDs is multifold. In terms of performance, functionalization with PEG200 and mercaptosuccinic acid yielded fluorescent CDs with an average size of 267 nm, maximum excitation at 320 nm, and peak emission at 430 nm. The fluorescence intensity of these dots is affected by the solvent, pH (showing an apparent pKa of 7.4), and iodide, which causes dynamic quenching but is not impacted by other metal ions such as Hg, Cu, Cd, Ni, and Zn. The fluorescence lifetimes have three complex decay components at around 2.7 ns, 7.4 ns, and 0.4 ns, and these lifetimes are not influenced by the PEG200 chain length nor the addition of mercaptosuccinic acid. In addition, PEGylation allows the carbon dots to be further functionalized with other molecules like mercaptosuccinic acid to develop novel nanosensors.

Small bioactive ligands like folic acid [93], hyaluronic acid [94], glucose [95], arginine-glycine-aspartic acid (RGD) peptide [96] and many more have also been integrated to instill CDs with sensitivity for overexpressed cancer biomarkers and related metabolic dysregulation. Amino acids like L-aspartic acid impart intrinsic brain cancer-targeting ability as elaborated by Zulfajri et al. [97]

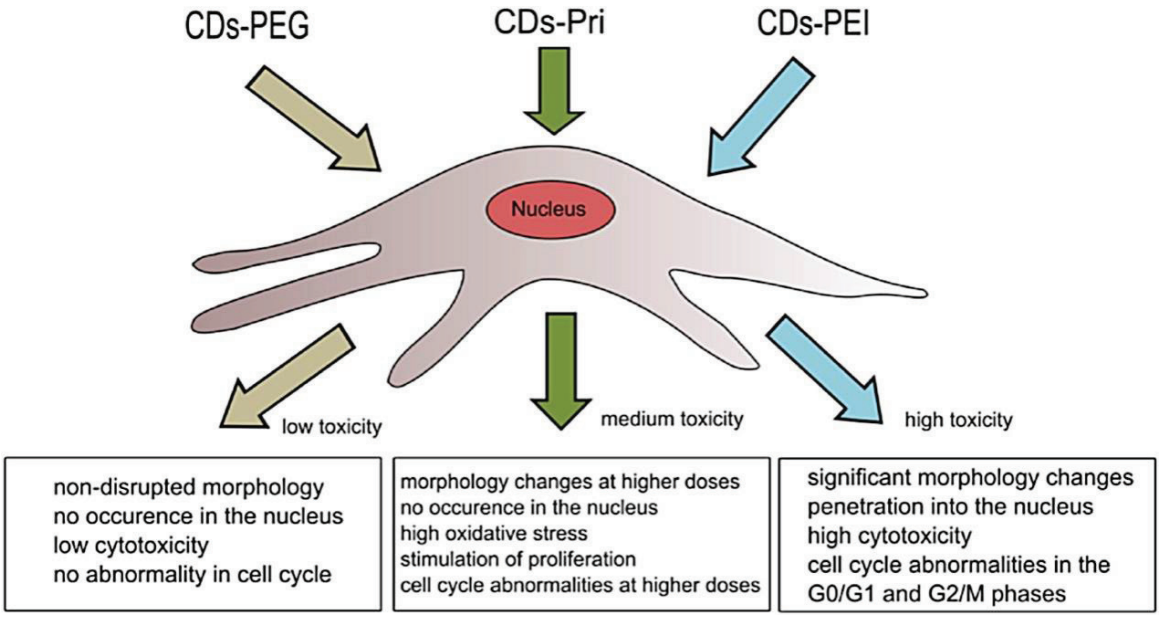

Fig. 5. Toxic effects of carbon dots with different surface chemistry [86]

The incorporation of such targeting ligands activates uptake mechanisms, like receptor-mediated endocytosis, for selective tracing of diseased cells overexpressing them.

4.3. Bioconjugation for targeted imaging and sensing

Surface functionalized CDs can be further bioconjugated with marker-specific recognition elements like antibodies, aptamers, and affinity molecules to selectively tag desired cells and biomolecules for sensitive optical detection. Immobilization of such biorecognition probes transforms CDs into targeted imaging contrast agents.

Antibodies that selectively bind corresponding cell surface protein antigens have been conjugated on CDs for specific cell labeling applications. For example, CDs chemically grafted with anti-EpCAM and anti-CD44 antibodies allowed differentiating epithelial vs mesenchymal type cancer cells overexpressed with the respective biomarkers [98, 99]. For example, Li et al. [100] developed a multifunctional nanoparticle called anti-EpCAM@PDA-CDs@Pt(IV) that combines imaging, targeted drug delivery, and chemo-photothermal therapy for treating liver cancer cells. The nanoparticles were made by attaching an antibody called anti-EpCAM and a chemotherapy drug called Pt(IV) to polydopamine CDs (PDA-CDs). Anti-EpCAM enabled targeted delivery to liver cancer cells that overexpress the EpCAM protein, while the PDA-CDs allowed fluorescence imaging to track the nanoparticles (Fig. 6A). The researchers showed that anti-EpCAM@PDA-CDs@Pt(IV) nanoparticles exhibited strong fluorescence for bioimaging, with high stability across varying pH and ionic concentrations. *In vitro* tests demonstrated targeted uptake in liver cancer cells and significant cytotoxicity triggered by near-infrared light irradiation attributed to combined chemo and photothermal therapy. *In vivo* results in a mouse model revealed targeted tumor accumulation and an 87.6% tumor growth inhibition rate through the synergistic treatment, higher than either chemotherapy or photothermal therapy alone. Histological analyses confirmed the destruction of tumor tissue without noticeable toxicity in other organs.

In addition to protein-based agents, oligonucleotide affinity molecules like aptamers also offer attractive probes for functionalizing CDs to generate targeting effects. Aptamers undergo conformational changes in the presence of the target,

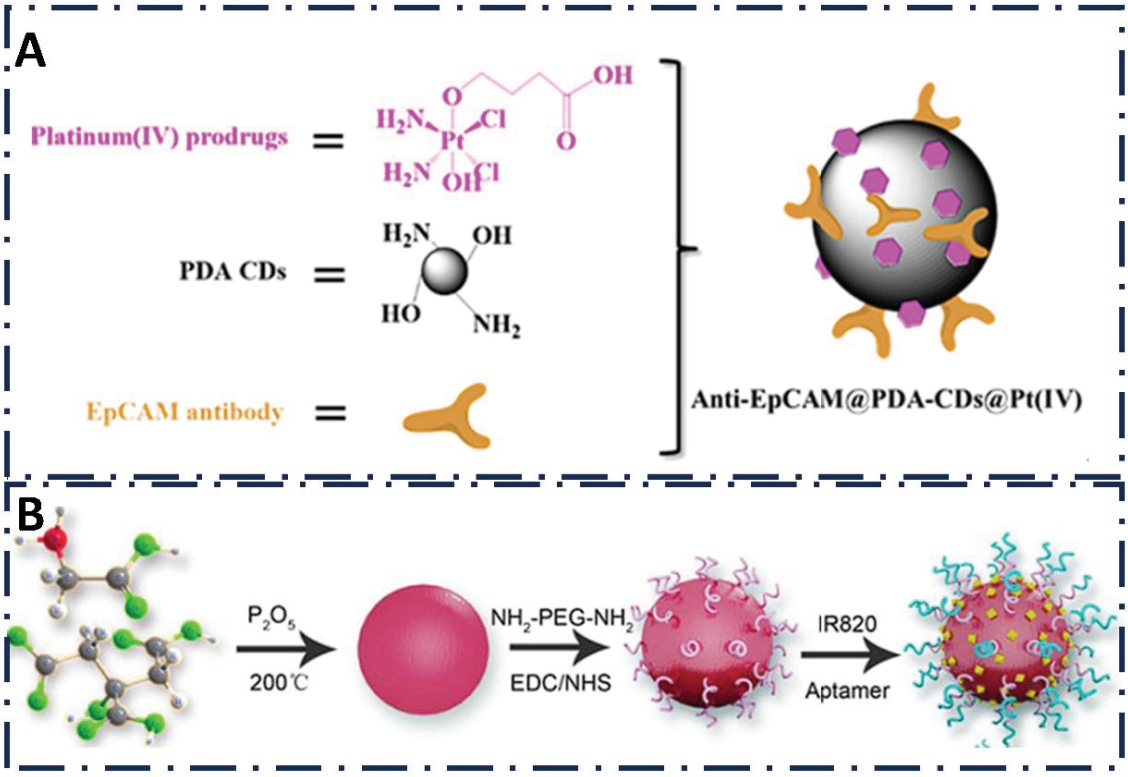

Fig. 6. (A) Schematic Illustration of Preparation of Anti-EpCAM@PDA-CDs@Pt(IV) [100]; (B) Schematic design of the assembly of the photoactive CDs-IR820-Aptamer nanomedicine [102]

modulating the quenching efficiency of adjacent fluorophores [101]. Liu et al. [102] developed a new nanomedicine called CD-IR820-Aptamer (Fig. 6B) made of carbon dots, IR820 dye, and an anti-vascular endothelial growth factor (VEGF) aptamer. They showed that this nanomedicine could selectively target tumor cells overexpressing VEGF receptors. Once taken up by cancer cells, the nanomedicine is localized to the mitochondria. When irradiated with an 808 nm near-infrared laser, the nanomedicine generated reactive oxygen species through type I photodynamic therapy, singlet oxygen through type II photodynamic therapy, and heat through photothermal therapy. Unlike traditional photodynamic therapies relying on singlet oxygen, this multifunctional nanomedicine retained efficacy even under hypoxic conditions *in vitro* and *in vivo*. In mouse models of breast cancer, the combination treatment of laser irradiation plus intravenous injection of CD-IR820-Aptamer resulted in significant tumor growth inhibition and damage compared to laser plus carbon dots or laser plus IR820 dye alone.

5. *In Vitro* Bioimaging Applications

5.1. CDs uptake, localization, and imaging in various cell lines

In vitro cell labeling, tracking intracellular fate, and organelle imaging applications constitute the most widely investigated implementations of fluorescent CDs before potential *in vivo* adoption. Due to innate size-dependent uptake and lack of specificity, most pristine CD preparations exhibit panspecific staining of standard cell lines. Hence, strategies rely on conjugation with targeting vectors for selective imaging.

Intrinsic endocytic internalization allows the majority of sub-10 nm sized CDs to spontaneously permeate plasma membranes and localize inside cells. For example, Rai et al. [103] reported a green

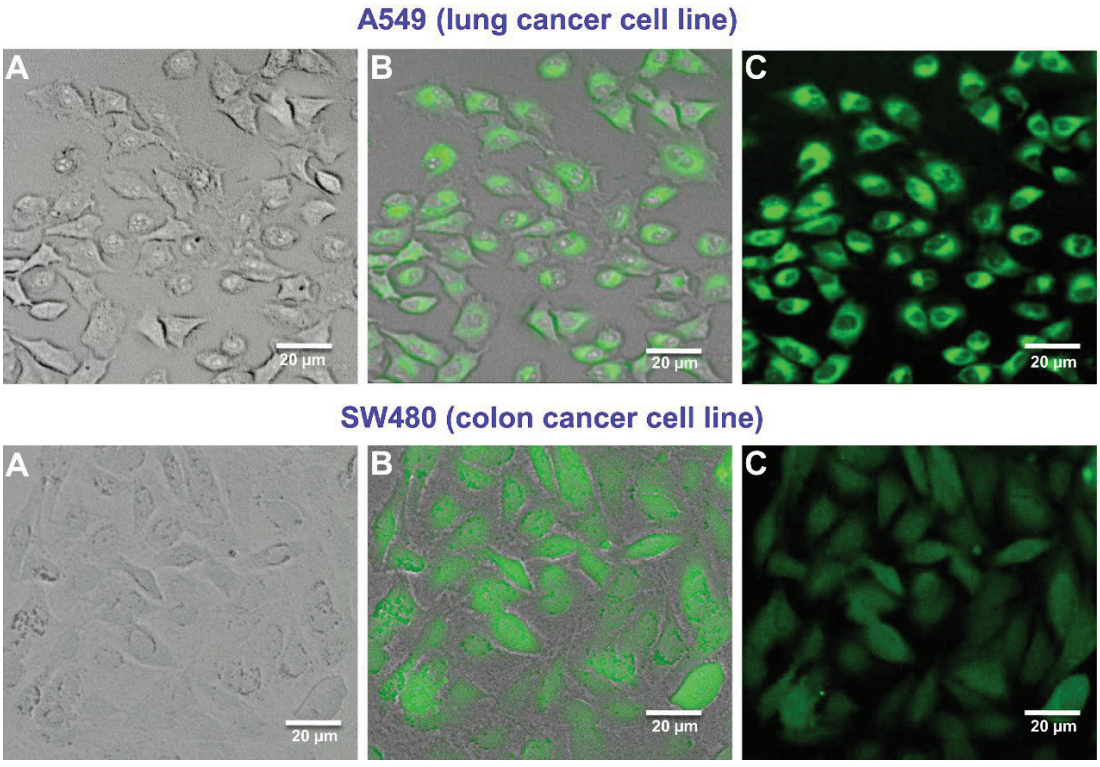

Fig. 7. Confocal fluorescence microscopy images of cancerous cells (A549 & SW480) labeled with prepared reduced fluorescent carbon dots, A (bright field), B (an overlay image of A & B) and C (excitation at 488 nm) (103)

method to synthesize reduced fluorescent CDs (r-FCDs) from lignosulfonate lignin using microwave irradiation. The resulting r-FCDs had an average diameter of 4.9 nm and maximum photoluminescence intensity at 475 nm when excited at 440 nm. The quantum yield was 47.3%. The r-FCDs showed high stability over a wide pH range and in saline solutions. The r-FCDs were incubated with A549 and SW480 cancer cell lines, and imaging showed cytoplasmic and nuclear localization, indicating cellular uptake (Fig. 7). The hemolysis assay demonstrated low toxicity, with only 2.89% hemolysis at 0.5 mg/mL r-FCDs concentration. Vasimalai et al. [70] synthesized CDs from four common spices - cinnamon, red chili, turmeric, and black pepper—using a green one-pot hydrothermal method. The CDs showed high fluorescence quantum yields of up to 43.6%, with particle sizes around 3–4 nm measured by TEM. The authors systematically evaluated the cytotoxicity and bioimaging potential of these spice-derived CDs *in vitro* using human glioblastoma cancer cells (LN-229) and non-cancerous human kidney cells (HK-2). The CDs exhibited differential toxicity in the cancer and non-cancer cells. After 24 hours of exposure, the spice CDs, especially those from black pepper, inhibited LN-229 cancer cell viability in a concentration-dependent manner, with 2 mg/mL yielding 35-75% growth inhibition. However, the CDs showed negligible toxicity in HK-2 cells. Confocal imaging demonstrated higher cellular uptake and cytoplasmic accumulation of spice C-dots in LN-229 versus HK-2 cells. Control citric acid CDs did not affect the viability of either cell type. The results suggested that spice CDs, particularly from turmeric and black pepper, have potential therapeutic applicability as cancer-targeting bioimaging agents with minimal toxicity to normal cells.

In terms of the subcellular distribution, the majority of naked anionic CDs localize in the cytoplasm and peri-nuclear spaces. Cationic CDs

with amine enrichment demonstrate higher nuclear affinity due to electrostatic attractions for negatively charged DNA and better permeation through nuclear pores. For example, Zhang et al. [104] synthesized NCDs via a one-step hydrothermal method. Characterization showed the NCDs had small size (4.35 nm), bright green fluorescence, abundant surface functional groups, and excellent fluorescence stability. The NCDs also demonstrated good biocompatibility with low cytotoxicity. When incubated with HeLa and PC12 cells, the NCDs could rapidly and specifically stain the nucleoli without needing additional washing steps. Further tests revealed the NCDs had a strong binding affinity to ribonucleic acid (RNA) abundant inside nucleoli, significantly enhancing NCD fluorescence. Digesting cellular RNA using ribonuclease inhibited NCD nucleoli staining, confirming the fluorescence enhancement mechanism. Similarly, Sachdev et al. [105] developed a dual-functional nanocomposite made of fluorescent CDs decorated on silver-zinc oxide nanoparticles (CDs-Ag@ZnO NCs) and evaluated its performance for bioimaging in cancer cells. The intrinsic fluorescence of the CDs allowed real-time monitoring of cellular uptake and localization of the NCs in MCF-7 breast cancer and A549 lung cancer cells using fluorescence microscopy, with higher uptake and nuclear localization observed compared to normal cells. The CDs served as an effective alternative to conventionally used organic dyes for tracking intracellular nanoparticle trafficking.

5.2. Targeted cell imaging: cancer, stem cells, neurons, etc.

While pristine CDs permit bulk staining of cells, surface engineering with targeting ligands imparts selectivity for discriminatory recognition of cancer cells, stem cells, and neurons. Taking clues from *in vitro* assays, the approach can be eventually translated to identify diseased tissues in more complex *in vivo* environments.

Cancer cell imaging applications leverage the binding of overexpressed surface biomarkers like folate receptors, hyaluronic acid, EpCAM, and mucins, as well as aberrant pH and protease microenvironments. Glycosylated liposomes conjugated CDs showed preferential labeling of HepG2 correctly reporting on metabolic dysregulation [106]. Mohammadi et al. [107] developed a highly sensitive ratiometric fluorescence assay for microRNA-21 detection using a nanohybrid of blue-emitting CDs (B-CDs) and yellow-emitting CDs (Y-CDs). The B-CDs were functionalized with a DNA probe to specifically recognize the microRNA-21 target. In the presence of microRNA-21, the fluorescence intensity of B-CDs at 410 nm decreased due to the inner filter effect, while the intensity at 540 nm increased. Using the ratio of fluorescence intensity change ($\Delta F540/\Delta F410$) as readout, the assay demonstrated a wide linear detection range of 0.15 fM to 2.46 pM and an ultralow detection limit down to 50 aM for microRNA-21. The assay could also quantify intracellular microRNA-21 in MCF-7 cancer cells over a range of 3,000 - 45,000 cells/mL (Fig. 8). Ratiometric CD probes targeted to cathepsin protease biomarkers also helped differentiate cancerous over normal cells by selective fluorescence light-up [108]. Through growth factor analog decoration, Shu et al. [109] traced HER2 receptors among the SK-BR-3 family, enabling the differentiation of breast cancer lines. Such surface re-engineering allows moving beyond panstaining towards molecular discrimination vital for cytological applications.

5.3. Organelle specific imaging: nucleus, mitochondria, and lysosomes

Beyond cell-level recognition, targeted delivery of CDs to intracellular organelles like the nucleus, mitochondria, and lysosomes allows probing their microenvironments and associated enzymatic activities [110]. Aberrations therein are linked with diseases, including cancer progression, making stimuli-responsive organelle imaging important.

Due to strong Coulombic affinity towards negatively charged macromolecules, amine-rich cationic CDs demonstrate natural nuclear localization abilities. For example, yellow emissive zwitterionic CDs prepared by citric acid permeated cell

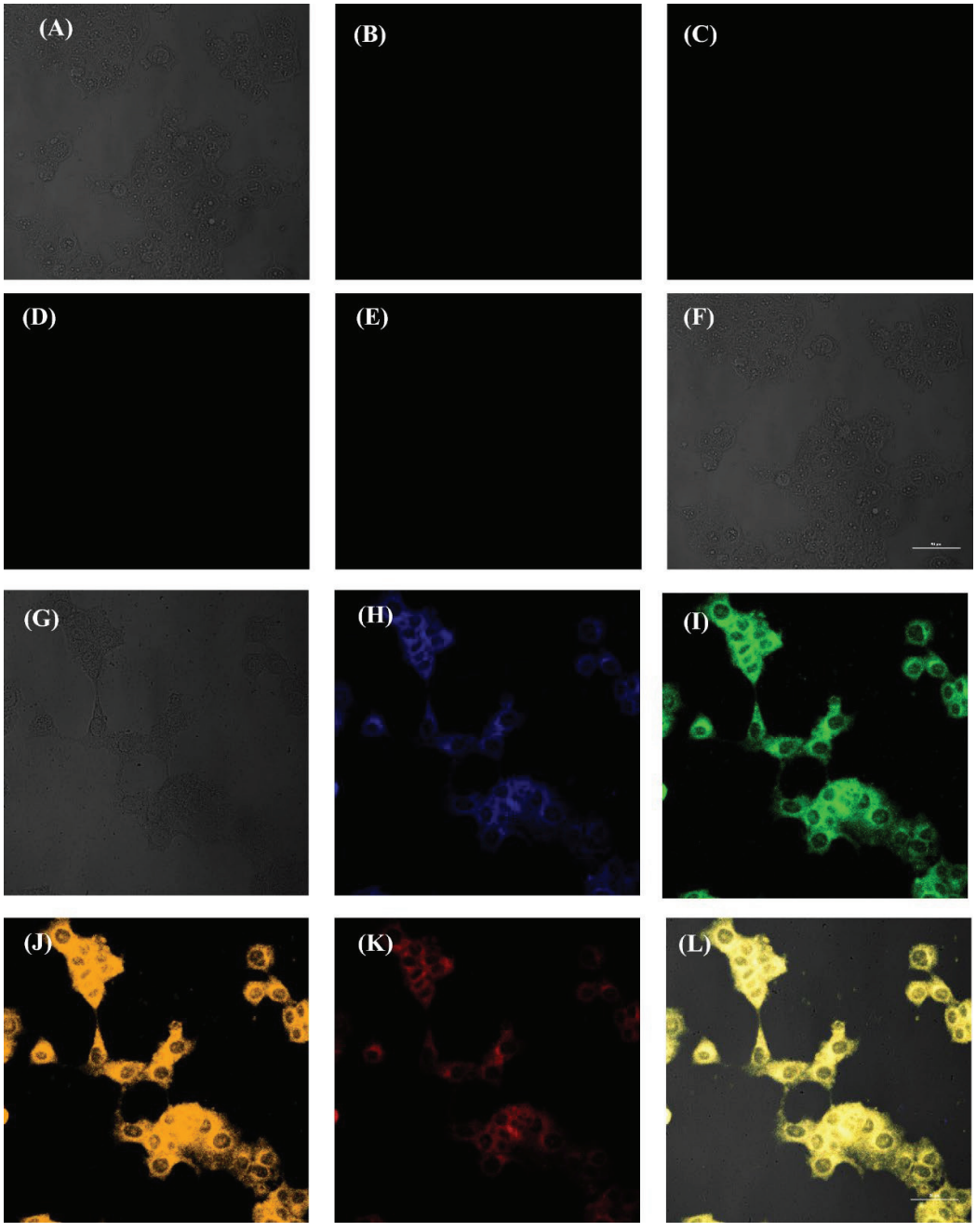

Fig. 8. Confocal laser scanning microscopic images of MCF-7: control (A–F) cells and cells treated with 1.0 mg/mL of BY-CDs (G–L) excitation by bright field (A, G), Blue (B, H), Green (C, I, Yellow (D, J), Red (E, K) and Merge (F, L) (107)

and nuclear membranes within 2 h [111]. Clear nucleolar binding permitted monitoring rRNA transcription activities via selective quenching interactions (Fig. 9A) [112]. Through conjugation with DNA intercalators like propidium iodide, CDs platforms also enable real-time monitoring of drug uptake for nuclear delivery applications (Fig. 9B) [113].

Mitochondria, being the powerhouse and metabolic signaling center, contributes to the initiation and progression of disorders, including neurodegeneration and tumorigenesis. Geng

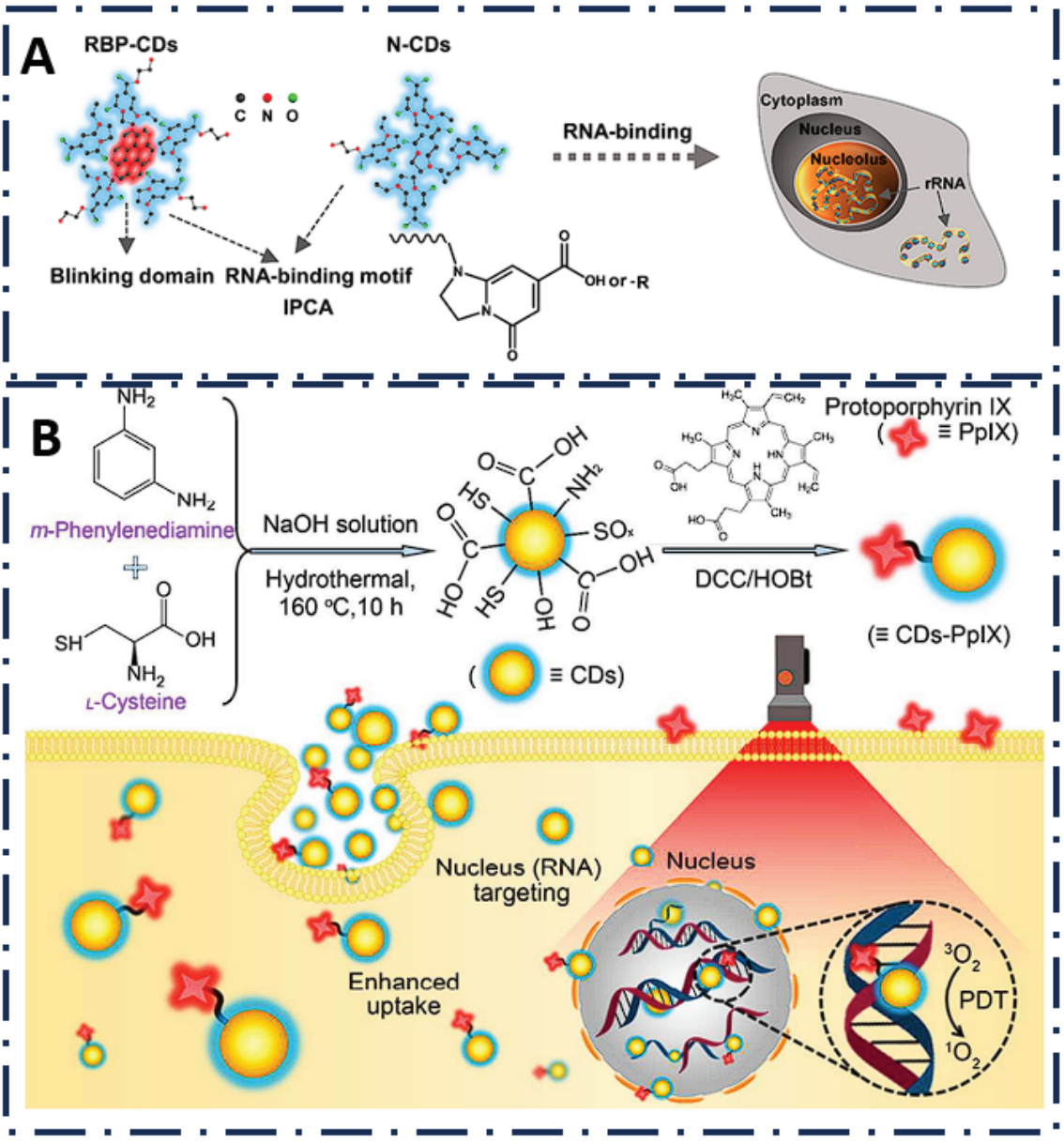

Fig. 9. (A) Schematic structures of RBP- and N-CDs for nucleolar imaging [112]; (B) Schematics of the synthetic procedure of CDs and selective nucleolus imaging of CDs [113]

et al. [114] developed mitochondria-targeted CD (MitoTCD) with tunable long-wavelength fluorescence ranging from green to red. The MitoTCD were synthesized via a retrosynthesis approach using citric acid and m-aminophenol derivatives as precursors. This allowed the incorporation of rhodamine as a luminescent center into the CDs. Four types of MitoTCD were made emitting at 520, 540, 580, and 600 nm with high quantum yields of 0.39, 0.44, 0.25, and 0.40, respectively (Fig. 10A). Targeted cellular imaging experiments demonstrated the MitoTCD could selectively localize to the mitochondria of HeLa cells after 4 h of incubation. Taking the MitoTCD 580 as an example, it was found to be independent of membrane potential and could continuously track the mitochondria for as long as six cell passages, indicating suitability for long-term imaging. Guo

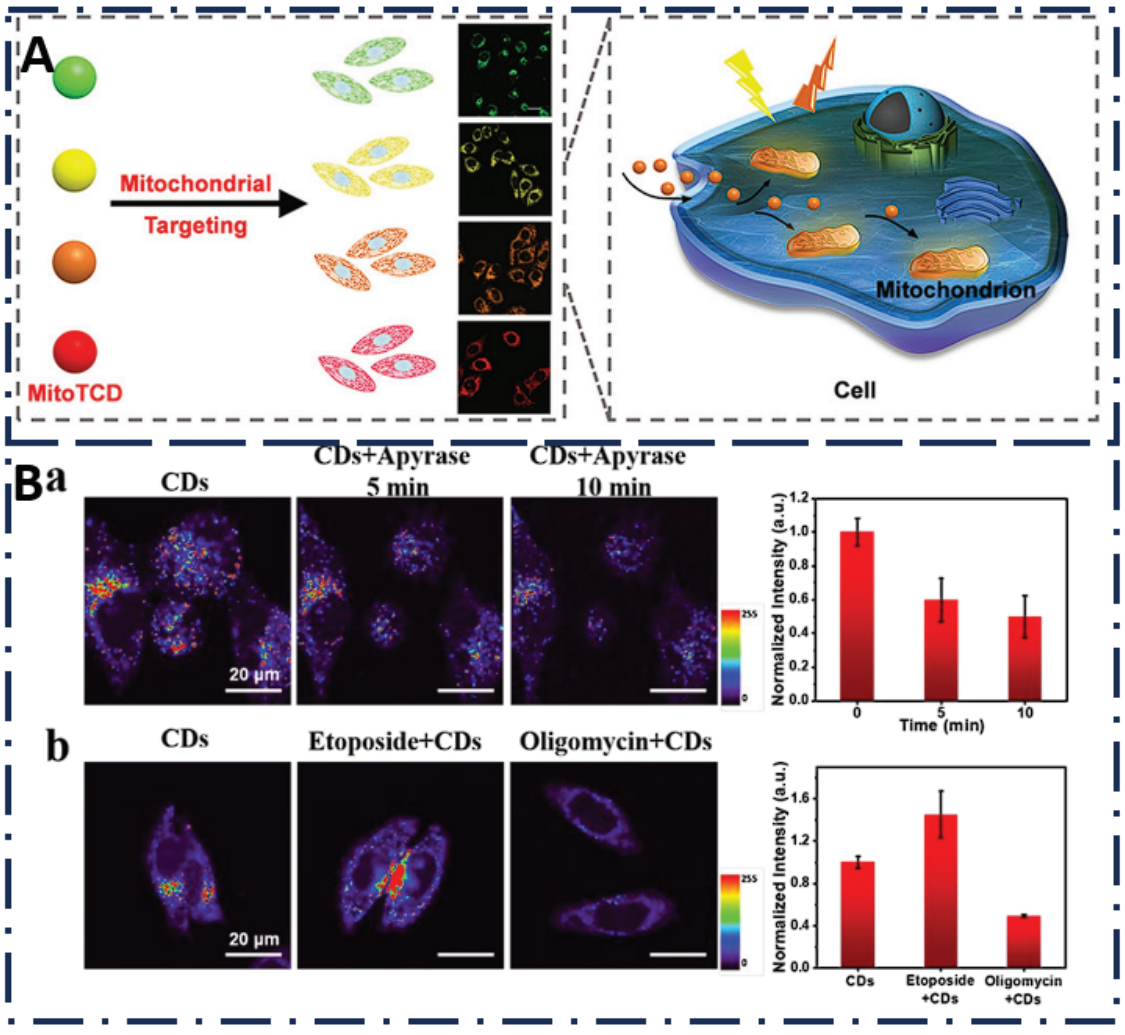

Fig. 10. (A) The application of MitoTCD in mitochondria imaging [114]; (B) (a) Fluorescent images of HepG-2 cells treated with 50 μg/mL CDs for 1 h and apyrase for 0, 5, and 10 min. (b) Fluorescent images of HepG-2 cells incubated with CDs, etoposide and CDs, or oligomycin and CDs [116]

et al. [115] synthesized fluorescent CDs that could shuttle between mitochondria and the nucleolus to visualize cell viability. In healthy cells, the positively charged CDs accumulated in the negatively charged mitochondria. However, when cells were damaged and the mitochondrial membrane potential decreased, the CDs migrated to the nucleolus, likely due to electrostatic interactions with nucleic acids concentrated there. Adding hydrogen peroxide damaged the cells and caused CD migration to the nucleolus, with the fluorescence intensity ratio of nucleus to cell increasing from 0.29 to 0.57. Subsequent addition of the antioxidant ascorbic acid recovered cell viability, causing the CDs to move back to the mitochondria, and the fluorescence ratio decreased to 0.32. Thus, the study demonstrated CDs that act as in situ visual reporters of cell viability based on their dynamic migration between cellular compartments.

In addition, abnormal lysosomal enzymes and upregulated catabolism also mark pathological transformations. Geng et al. [116] developed fluorescent CDs that can detect adenosine triphosphate (ATP), specifically within acidic lysosomes in cells. In acidic solutions (pH 4.5-5.5) resembling the lysosomal environment, the CDs exhibited a

yellow fluorescence when they interacted with ATP. This on-off fluorescence switching enabled selective detection of ATP within lysosomes without signals from ATP in the neutral pH cytoplasm or other organelles. The CDs had a linear ATP detection range from 0.01 to 0.3 mM ATP. When applied to human cancer cell lines, the CDs demonstrated colocalization with a commercial lysosome dye, indicating lysosome-specific accumulation. Further, the CDs' fluorescence intensities changed in response to drugs that modulated intracellular ATP levels and lysosomal pH/integrity over time (Fig. 10B).

6. *In Vivo* Bioimaging Applications

6.1. Biodistribution and pharmacokinetics

Translation of CDs utility from *in vitro* assays to *in vivo* administration mandates studies into pharmacokinetic fate and biodistribution trends for evaluating safety. Key considerations encompass circulation half-life, preferential accumulation, metabolism, and clearance pathways, which impact toxicity concerns- especially for therapeutic modalities like drug delivery and phototherapy.

Pioneering research reveals renal clearance as the predominant elimination pathway for intravenously injected CDs with peak signal from the bladder evident in small animals within an hour of injection [117]. The renal filtration cut-off of around 10 nm allows the elimination of sub-10 nm CD particulates. Analyses reveal gradual release over 12–24 hours with negligible toxicity via the fecal route, too (Fig. 11) [118]. However, surface PEGylation and charge modulation variably prolong circulatory residence time compared to anionic raw CDs, which undergo rapid opsonization. Metabolic fate through enzymatic breakdown into constituent biomolecules minimizes risks of bioaccumulation upon chronic exposures [119].

In terms of biodistribution, Yang et al. [120] investigated the toxicity and biodistribution of CDs in mice after a single inhalation exposure. CDs were synthesized by hydrothermal method and characterized. Mice were exposed by inhalation to CDs at doses of 5, 2 and 1 mg/kg. Results showed CDs caused dose-dependent mortality, with 14% mortality at the highest dose after 15 days. Blood analysis indicated CD-induced inflammation. Liver enzymes were elevated in a dose-dependent manner, suggesting liver damage. The fluorescent intensity of lung and liver homogenates increased in a time-dependent fashion over 28 days, indicating accumulation of CDs over time. In contrast, kidney intensity peaked at one day and then declined, suggesting clearance of CDs. Histopathology and TEM confirmed lung and liver injury but no brain damage. Lung effects included inflammation, edema, and epithelial cell vacuolation. Liver effects included necrosis and cytoplasmic vesiculation of Kupffer cells from CD phagocytosis. Huang et al. [121] investigated how different injection routes, intravenous (IV), subcutaneous (SC), and intramuscular (IM), affected the biodistribution, clearance, and tumor uptake of fluorescent CDs in mice (Fig. 12). The CDs were labeled with the near-infrared dye ZW800 to allow tracking by optical imaging. Blood circulation analysis found that IV injection resulted in the fastest clearance, with blood levels 17-fold lower at 60 minutes post-injection than at one minute. SC and IM injection showed slower clearance, with blood levels increasing up to 30 min before plateauing. Biodistribution studies showed the majority of CDs accumulated in the kidneys by 1 h post-injection, indicating renal clearance. By 24 h, CDs were completely cleared from the body by all routes. Urine analysis confirmed IV injection had the fastest clearance, with fluorescence plateauing after 10 min. Tumor uptake was higher in the IV and SC groups compared to IM at 2 h, likely due to the interplay between circulation time, clearance rate, and particle concentration.

6.2. Tumor targeted imaging, crossing blood-brain barrier

Surface functionalized CDs grafted with targeting ligands selectively accumulate in tumors by binding overexpressed receptors on cancer cells. Cross-recognition hence amplifies signal contrast for sensitive diagnosis. In parallel, specific

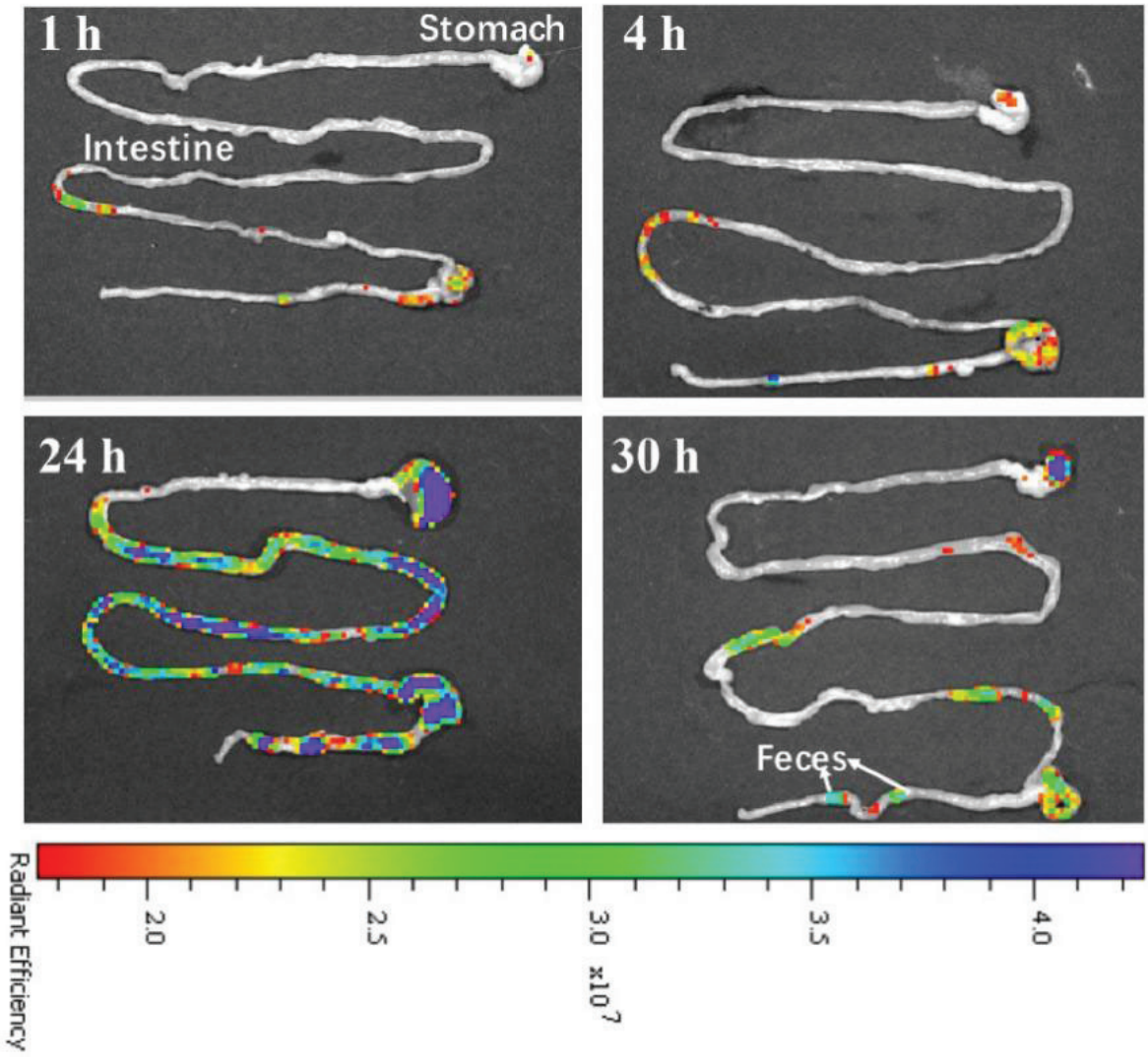

Fig. 11. Fluorescent images of the *ex vivo* stomach and intestine from mice injected with CDs@PEI nanoparticles at 1, 4, 24, and 30 h [118]

oligopeptides also enable permeation across tight blood-brain barrier junctions for neural imaging.

Due to the enhanced permeability and retention effect of leaky tumor vasculature, pristine CDs display some passive uptake, too. However, conjugation with homing elements provides active facilitation via ligand-receptor binding events. Common targeting motifs used include cyclic RGD peptides for recognizing $\alpha v\beta 3$ integrins, folic acid to interact with folate receptors, and antibodies identifying accessible cancer antigens. Liu et al. [122] successfully developed integrin $\alpha v\beta 3$-targeted CDs nanocomposites called MB-CDs@NH-RGD. Soybean milk was used as a green carbon source, along with methylene blue and TTDDA, to fabricate the CDs. Surface modification via TTDDA coating and RGD peptide conjugation endowed the nanocomposites with superior biocompatibility and highly specific targeting to $\alpha v\beta 3$-overexpressed breast cancer and melanoma cell lines. A significant photothermal effect was generated when targeted CD nanocomposites were irradiated with a pulsed laser, proving their potential for thermal ablation therapy. *In vivo*, photoacoustic imaging using nanocomposites as contrast agents showed excellent targeting sensitivity and enhancement.

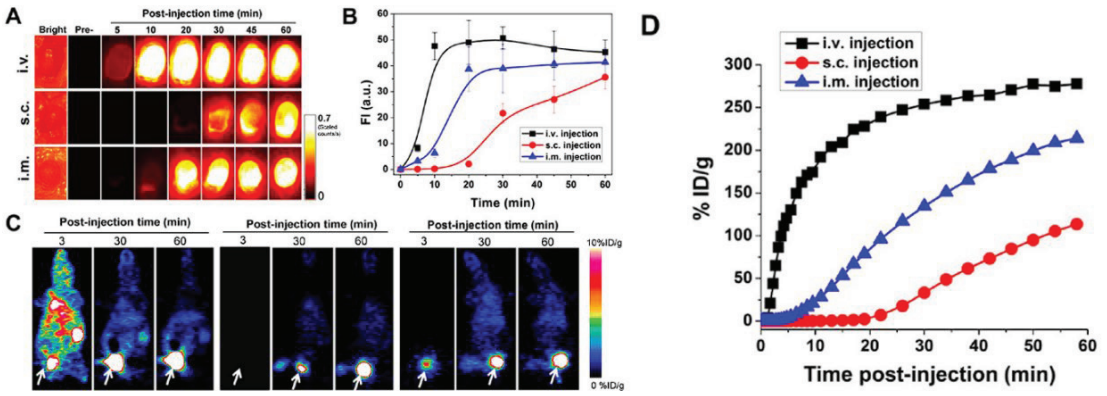

Fig. 12. Urine accumulation of CDs-ZW800 after different routes of injection. (A) The mice were kept under isoflurane anesthesia, the bladder was exposed, and NIR images were acquired at the indicated time points before and after (top) IV injection, (middle) SC injection, and (bottom) IM injection; (B) Quantification of the ZW800 fluorescence signal in (A); (C) Representative coronal images from 1 h dynamic PET imaging of 64Cu-CDs after three routes of injection: left, IV injection; middle, SC injection; right, IM injection; (D) Urinary bladder ROI analysis of the PET images in (C) [121]

Cytotoxicity assays found the modified nanocomposites had better biocompatibility and lower toxicity than non-modified counterparts in cancer cell lines. Dual-channel fluorescence imaging verified targeted nanocomposite internalization and labeling of cancer cells via receptor-mediated endocytosis. Confocal microscopy imaging demonstrated that cancer cell lines overexpressing the folate receptor (HeLa, SKOV3) were strongly labeled by the folic acid CDs through folate receptor-mediated uptake [123]. Cell lines with medium or low folate receptor expression (HepG2, MCF7) showed moderate labeling, while lines lacking the receptor (CHO, A549) displayed negligible labeling. Competition experiments with free folic acid reduced cell labeling in a concentration-dependent manner.

In parallel, crossing the tightly packed blood-brain barrier (BBB) endothelium remains a huge challenge for conventional imaging agents and therapies against aggressive cancers like glioblastoma. Unique oligopeptides conjugated over CDs facilitate transport across this barricade to neural cells. For instance, the glucose-based CDs (GluCDs) and conjugated them with fluorescein (GluCDs-F) to test their ability to cross the BBB *in vivo* [124]. They first showed that the cellular uptake of GluCDs in yeast cells requires glucose transporters, suggesting the GluCDs enter cells through glucose transporter proteins. They then injected GluCDs-F intravascularly into the hearts of zebrafish and observed accumulation in the central nervous system, indicating successful BBB passage. Similarly, intravenous injection of GluCDs-F in rats led to its presence in the brainstem and spinal cord grey matter 4 h later, consistent with neuronal localization. The absence of GluCDs-F in white matter suggested limited axonal transport. Together, these findings demonstrated that GluCDs can cross the BBB without additional targeting ligands and carry small molecule cargo into the central nervous system in both zebrafish and mammalian models (Fig. 13). As neuron targeting drug delivery platforms, GluCDs may have promising therapeutic potential for neurodegenerative diseases, spinal cord injuries, and brain malignancies.

6.3. Image-guided drug delivery and cancer therapy

Leveraging their long circulation and tumor-homing abilities, theranostic CDs platforms loaded with chemotherapeutic payloads enable tracking delivery to improve efficacy and safety. Light-triggered unloading of drugs/proteins additionally

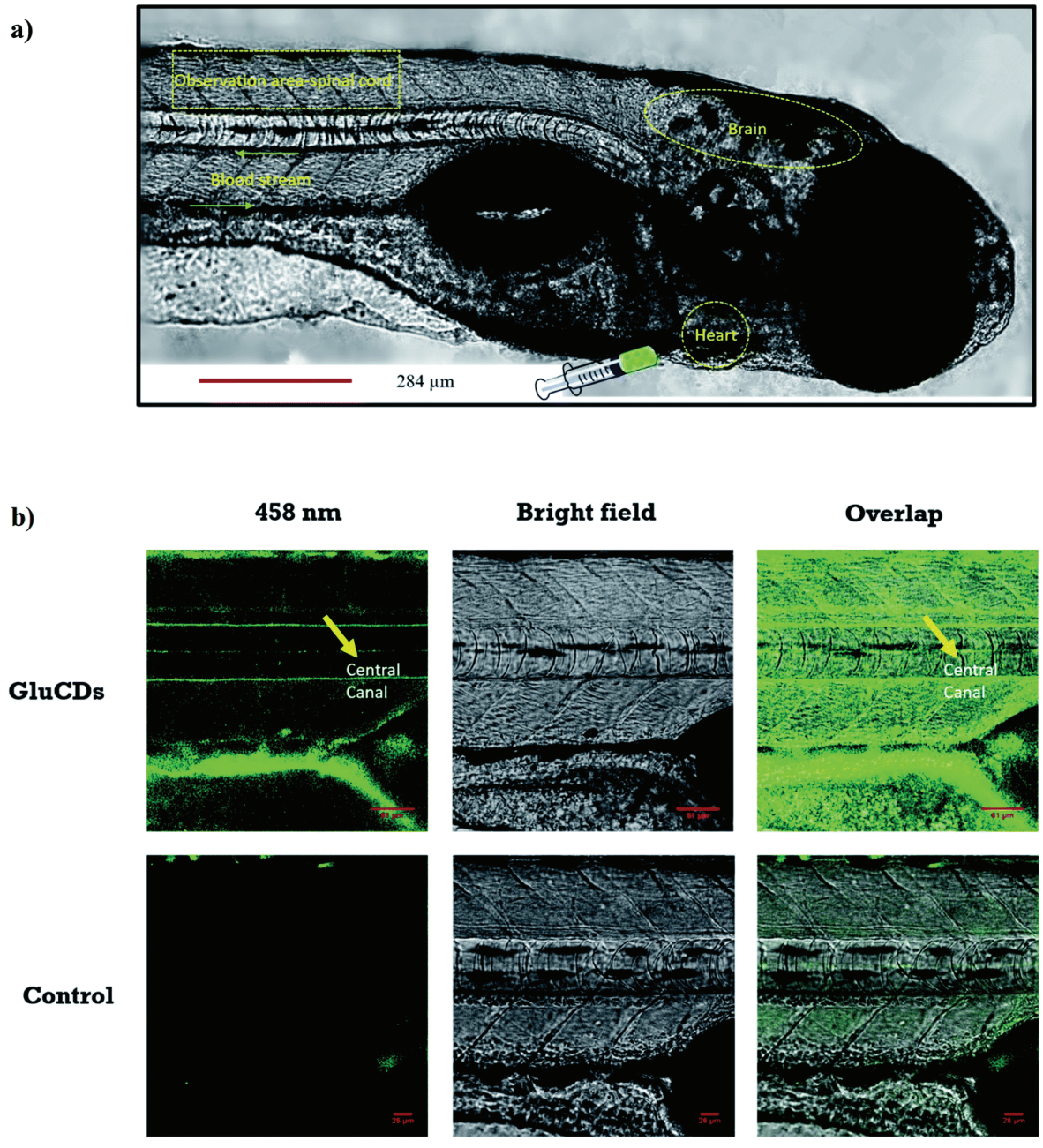

Fig. 13. (a) Confocal images of wild-type zebrafish showing the injection route, heart, blood stream, CNS and observation area (central canal of spinal cord); (b) Accumulation of GluCDs-F in the CNS of zebrafish. The yellow arrow indicates the central canal of spinal cord of zebrafish [124]

grants spatiotemporal control for site-specific therapy with imaging feedback.

By exploiting the enhanced permeability and retention effect, nanoparticles passively permeate and accumulate in tumor interstitium enhancing local concentrations of cargo like doxorubicin (DOX) and paclitaxel for greater apoptosis. Yuan et al. [125] developed a drug delivery system using CDs synthesized from milk to carry the chemotherapy drug DOX. The CDs were characterized as small (less than 10 nm), hydrophilic particles with oxygen and carboxyl surface groups. DOX was

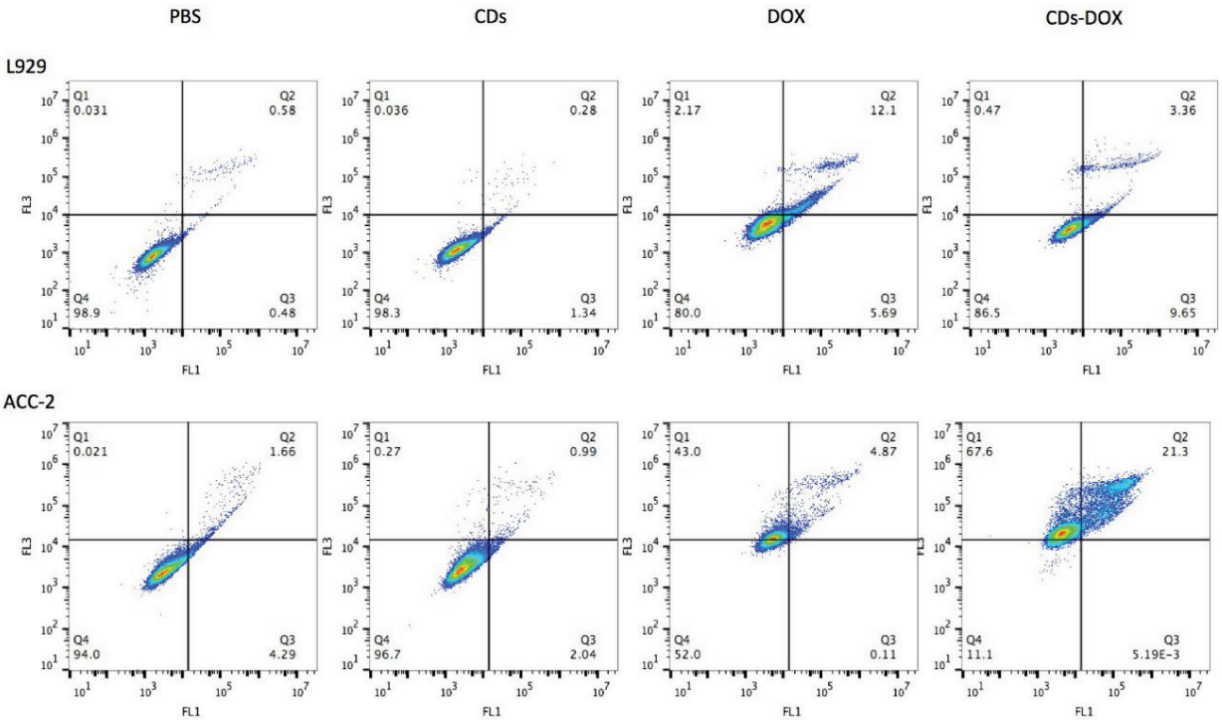

Fig. 14. Apoptosis analysis. The L929 cells and the ACC-2 cells were incubated with PBS, CDs (200 μg/mL), free DOX and CDs-DOX (at the same DOX concentration, 1.5 μM) for 48 h. Then the cells were stained by PI and Annexin V-FITC, flowed by flow cytometry (125)

successfully loaded onto the CDs through electrostatic interactions with 87% efficiency. *In vitro* tests showed the CDs-DOX complexes released more DOX in acidic conditions similar to the tumor microenvironment compared to neutral pH. Cell studies found the CDs were non-toxic, while the CDs-DOX complexes showed enhanced toxicity against human adenoid cystic carcinoma cells compared to free DOX. The CDs-DOX complexes are localized in the cell nucleus due to interactions between the CDs and the nuclear membrane. Flow cytometry indicated the CDs-DOX complexes had slower uptake than free DOX but increased apoptosis of cancer cells (Fig. 14). Chowdhury and Das [126] developed a biotin-modified iron-doped CD (FCDsb) that can selectively sense, activate, and deliver anticancer drugs to cancer cells. FCDsb was synthesized via a hydrothermal method and surface functionalized with biotin to target biotin receptors overexpressed in cancer cells. FCDb exhibited blue fluorescence and could sense H_2O_2 in cancer cells by fluorescence quenching. In the presence of FCDsb, H_2O_2 generated reactive oxygen species that caused oxidative DNA damage. FCDsb showed higher cellular uptake and H_2O_2-mediated fluorescence quenching in cancer cells compared to normal cells. The anticancer drug paclitaxel was loaded onto FCDsb (FCDsb-PTX). FCDsb-PTX exhibited 2.7-3.5 fold higher killing of melanoma cancer cells compared to normal cells through a combination of H_2O_2-induced oxidative damage and paclitaxel's anticancer effects. Cancer cell death occurred via early and late-stage apoptosis.

7. Challenges and Future Outlook

7.1. Reproducibility and large-scale synthesis

Despite extensive strides, the adoption of CDs for practical applications faces roadblocks like batch-to-batch variability and a lack of robust, scalable green production routes. As an emerging

field, reproducibility issues plague the domain, with results heavily contingent on exact experimental conditions. The complex interplay of factors like precursor nature, process conditions, and work-up protocols, unlike small organic dyes, leads to intricacies in duplicated production.

Moreover, current laboratory-scale syntheses demand extensive inputs of solvents, time, and infrastructure, precluding commercial adoption. For instance, hydrothermal methods employ corrosive acids and bases alongside high temperatures and pressures. Microwave and ultrasonication routes require specialized instrumentation, too [127]. Biocompatible production hence necessitates clean, high-yielding assembly strategies. Some beginnings have been made, like flow chemistry as well as sustainable bio-mediated and photochemical set-ups [128].

The intricacies mean products need extensive benchmarking and custom protocols developed by individual groups, unlike off-the-shelf dyes. Developing robust, environmentally benign scalable chimies for consistent, shape-controlled CDs with lasting usable fluorescence remains an important goal [129]. Taming the complex parametric interplays is vital to cement reproducibility.

7.2. Toxicity concerns and long-term effects

While most research corroborates the general biocompatibility of CDs, nagging concerns about long-term toxicity, especially for therapeutic applications like drug delivery, persist [130]. Troubling environmental health reports on graphene and carbon nanotubes, despite early promise, warrant cautionary adoption.

Issues like oxidative stress induction, bioaccumulation upon chronic exposures, and activation of inflammatory pathways need careful assessments across cell and animal models before clinical translation [131]. Unlike transient labeling applications, particle carriage of drugs and tenure in phototherapy mandates safety vetting with well-designed longitudinal trials and multi-parametric bioanalyses for formal toxicological profiling. Transport across BBB also warrants neuroimmune appraisal [132]. Terrestrial toxicology through simulated environmental releases also merits attention prior to manufacturing scale up to avoid unintended contamination similar to microplastics.

Standardized toxicity analysis frameworks, building risk-benefit matrixes spanning vector design variables, and emphasizing safe-by-design principles need community adoption prior to widespread endorsements for biomedical uses. Regulations need to balance innovation possibilities against ethical prerogatives.

7.3. New bioimaging modalities and biomedical applications

While fluorescence-based optical imaging constitutes the predominant implementation of CDs currently, other modalities like Raman spectroscopy [133], photoacoustics [134], radiolabeling [135], and integration with magnetic platforms offers uncharted possibilities.

For instance, surface-enhanced Raman scattering (SERS) tags based on gold-CD nanocomposites provide ultra-detection sensitivity and multiplexing capabilities for intracellular mapping unviable through fluorescence alone. Radio-labeled CDs similarly enhance penetration depths for whole-body analyses, as opposed to optical means limited by light scattering. Ultrasound and magnetic resonance interfacing also improve *in vivo* imaging capabilities in opaque anatomical niches.

In parallel, diverse clinical adoption avenues beyond common targeting, drug delivery, and phototherapy continue to emerge. Usage as contrast enhancers for surgical resection, theranostic dentistry, plant imaging, and food safety analysis illustrates expanding utility. Further clinical solutions for challenging applications like multiple sclerosis, cardiovascular imaging, immunotherapy, and central nervous system drug delivery will catalyze impact.

Building such multimodal, cross-domain partnerships by interfacing CDs with varied modalities, analysis tools, and application landscapes promises to usher in the next wave of biomedical solutions, fully harnessing their nanoscale versatility.

8. Conclusion

In conclusion, this review comprehensively summarizes recent advances in applying biosynthesized CDs as fluorescent probes for sensitive bioimaging. A variety of sustainable precursors, from natural extracts to waste biomaterials, can produce CDs with desirable properties like tunable visible to near-infrared emissions, large Stokes shifts, high quantum yields exceeding 50%, and excellent photostability. Careful optimization of key synthetic parameters allows for the customization of fluorescence features tailored to imaging needs. While crude CDs permit pan-cellular staining, surface passivation, and bioconjugation with polymers, small ligands and recognition elements like antibodies/aptamers instill target sensitivity towards entities ranging from cancer cells and subcellular organelles to disease biomarkers. *In vitro* validation across standard lines shows CDs' promise for superficial probing of biological interactions. Translation to *in vivo* administration reveals biodistribution trends like renal clearance and preferential tumor accumulation at sufficient levels for diagnostic imaging contrast. Overall, the intrinsic biocompatibility of top-down synthesized CDs compared to graphene/carbon nanotubes, coupled with abundant facile and eco-friendly production routes, offers renewed impetus. However, concerns regarding toxicity from chronic exposures, large-scale reproducible manufacturing, and multimodal imaging capabilities need redressal prior to further penetration. On the balance, CDs displayed between 36 and 87% tumor growth inhibition in mouse models, demonstrating good potential as sensitizers for precise fluorescence-guided drug delivery and therapy. The next wave of innovation harnessing CDs calls for synergistic alliances across domains spanning sustainable chemistry, materials science, biotechnology, and nanomedicine to develop solutions combating disease morbidity and environmental issues.

Conflict of Interest

The author declared no potential conflicts of interest with respect to the research, authorship, and/or publication of this article.

Acknowledgments

This work was supported by NSFC21867005, Guizhou Provincial Science and Technology Plan Project QKHP-TRC[2018]5769, Guizhou Provincial Science and Technology Program Project QKHJC[2020]1Y430, and Guizhou Province High-level Overseas Talents Selection Funding Project (2019)12.

References

[1] Li H, Yan X, Kong D, Jin R, Sun C, Du D, et al. Recent advances in carbon dots for bioimaging applications. *Nanoscale Horizons*. 2020;5(2):218–34.

[2] Carlson LJ, Krauss TD. Photophysics of individual single-walled carbon nanotubes. *Acc Chem Res*. 2008 Feb 1;41(2):235–43.

[3] Liu Y, Huang H, Cao W, Mao B, Liu Y, Kang Z. Advances in carbon dots: from the perspective of traditional quantum dots. *Materials Chemistry Frontiers*. 2020;4(6):1586–613.

[4] Zhu S, Zhang J, Wang L, Song Y, Zhang G, Wang H, et al. A general route to make non-conjugated linear polymers luminescent. *Chem Commun*. 2012 Oct 10;48(88):10889–91.

[5] Ghosal K, Ghosh A. Carbon dots: The next generation platform for biomedical applications. *Materials Science and Engineering: C*. 2019 Mar 1;96:887–903.

[6] Sagbas S, Sahiner N. 22 – Carbon dots: preparation, properties, and application. In: Khan A, Jawaid M, Inamuddin, Asiri AM, editors. *Nanocarbon and its Composites*. Woodhead Publishing; 2019 [cited 2024 Jan 31]. p. 651–76. (Woodhead Publishing Series in Composites Science and Engineering). Available from: https://www.sciencedirect.com/science/article/pii/B9780081025093000225

[7] Xu D, Lin Q, Chang HT. Recent advances and sensing applications of carbon dots. *Small Methods*. 2020;4(4):1900387.

[8] Gonçalves H, Jorge PAS, Fernandes JRA, Esteves da Silva JCG. Hg(II) sensing based on functionalized carbon dots obtained by direct laser ablation. *Sensors and Actuators B: Chemical*. 2010 Mar 19;145(2):702–7.

[9] Chao-Mujica FJ, Garcia-Hernández L, Camacho-López S, Camacho-López M, Camacho-López MA, Reyes Contreras D, et al. Carbon quantum dots by submerged arc discharge in water: Synthesis, characterization, and mechanism of formation. *Journal of Applied Physics*. 2021 Apr 22;129(16):163301.

[10] Liu M, Xu Y, Niu F, Gooding JJ, Liu J. Carbon quantum dots directly generated from electrochemical oxidation of graphite electrodes in alkaline alcohols and the applications for specific ferric ion detection and cell imaging. *Analyst*. 2016 Apr 25;141(9):2657–64.

[11] Meng W, Bai X, Wang B, Liu Z, Lu S, Yang B. Biomass-derived carbon dots and their applications. *Energy & Environmental Materials*. 2019;2(3):172–92.

[12] Wareing TC, Gentile P, Phan AN. Biomass-based carbon dots: current development and future perspectives. *ACS Nano*. 2021 Oct 26;15(10):15471–501.
[13] Mathew S, Mathew B. A review on the synthesis, properties, and applications of biomass derived carbon dots. *Inorganic Chemistry Communications*. 2023 Oct 1;156:111223.
[14] Long C, Jiang Z, Shangguan J, Qing T, Zhang P, Feng B. Applications of carbon dots in environmental pollution control: A review. *Chemical Engineering Journal*. 2021 Feb 15;406:126848.
[15] Ai L, Yang Y, Wang B, Chang J, Tang Z, Yang B, et al. Insights into photoluminescence mechanisms of carbon dots: advances and perspectives. *Science Bulletin*. 2021 Apr 30;66(8):839–56.
[16] Zhu S, Song Y, Zhao X, Shao J, Zhang J, Yang B. The photoluminescence mechanism in carbon dots (graphene quantum dots, carbon nanodots, and polymer dots): current state and future perspective. *Nano Res*. 2015 Feb 1;8(2):355–81.
[17] Zhou J, Yang Y, Zhang C. Toward biocompatible semiconductor quantum dots: from biosynthesis and bioconjugation to biomedical application. *Chem Rev.* 2015 Nov 11;115(21):11669–717.
[18] Carrillo-Carrion C, Parak WJ. Design of pyridyl-modified amphiphilic polymeric ligands: towards better passivation of water-soluble colloidal quantum dots for improved optical performance. *Journal of Colloid and Interface Science.* 2016 Sep 15;478:88–96.
[19] Fan Y, Liu H, Han R, Huang L, Shi H, Sha Y, et al. Extremely high brightness from polymer-encapsulated quantum dots for two-photon cellular and deep-tissue imaging. *Sci Rep.* 2015 Apr 24;5(1):9908.
[20] Zhou Y, Mintz KJ, Sharma SK, Leblanc RM. Carbon dots: diverse preparation, application, and perspective in surface chemistry. *Langmuir.* 2019 Jul 16;35(28):9115–32.
[21] Li S, Guo Z, Zhang Y, Xue W, Liu Z. Blood compatibility evaluations of fluorescent carbon dots. *ACS Appl Mater Interfaces.* 2015 Sep 2;7(34):19153–62.
[22] Peng Z, Ji C, Zhou Y, Zhao T, Leblanc RM. Polyethylene glycol (PEG) derived carbon dots: preparation and applications. *Applied Materials Today.* 2020 Sep 1;20:100677.
[23] Qian J, Quan F, Zhao F, Wu C, Wang Z, Zhou L. Aconitic acid derived carbon dots: conjugated interaction for the detection of folic acid and fluorescence targeted imaging of folate receptor overexpressed cancer cells. *Sensors and Actuators B: Chemical.* 2018 Jun 1;262:444–51.
[24] Wang L, Hu C, Shao L. The antimicrobial activity of nanoparticles: present situation and prospects for the future. *International Journal of Nanomedicine.* 2017;12:1227–49.
[25] Nel AE, Mädler L, Velegol D, Xia T, Hoek EM, Somasundaran P, et al. Understanding biophysicochemical interactions at the nano–bio interface. *Nature Materials.* 2009;8(7):543–57.
[26] Mahmoudi M, Lynch I, Ejtehadi MR, Monopoli MP, Bombelli FB, Laurent S. Protein–nanoparticle interactions: opportunities and challenges. *Chemical Reviews.* 2011;111(9):5610–37.
[27] Treuel L, Jiang X, Nienhaus GU. New views on cellular uptake and trafficking of manufactured nanoparticles. *Journal of the Royal Society Interface.* 2013;10(82):20120939.
[28] Yang K, Ma YQ. Computer simulation of the translocation of nanoparticles with different shapes across a lipid bilayer. *Nature Nanotechnology.* 2010;5(8):579–83.
[29] Raniszewski G, Pyc M, Kolacinski Z. Optimization of magnetic field-assisted synthesis of carbon nanotubes for sensing applications. *Sensors.* 2014 Oct;14(10):18474–83.
[30] Sidorov AI, Lebedev VF, Kobranova AA, Nashchekin AV. Formation of carbon quantum dots and nanodiamonds in laser ablation of a carbon film. *Quantum Electron.* 2018 Jan 1;48(1):45.
[31] Zhou J, Booker C, Li R, Zhou X, Sham TK, Sun X, et al. An electrochemical avenue to blue luminescent nanocrystals from multiwalled carbon nanotubes (MWCNTs). *J Am Chem Soc.* 2007 Jan 1;129(4):744–5.
[32] Du X, Zhang M, Ma Y, Wang X, Liu Y, Huang H, et al. Size-dependent antibacterial of carbon dots by selective absorption and differential oxidative stress of bacteria. *Journal of Colloid and Interface Science.* 2023 Mar 15;634:44–53.
[33] Huang H, Lv JJ, Zhou DL, Bao N, Xu Y, Wang AJ, et al. One-pot green synthesis of nitrogen-doped carbon nanoparticles as fluorescent probes for mercury ions. *RSC Advances.* 2013;3(44):21691–6.
[34] Pei S, Zhang J, Gao M, Wu D, Yang Y, Liu R. A facile hydrothermal approach towards photoluminescent carbon dots from amino acids. *Journal of Colloid and Interface Science.* 2015 Feb 1;439:129–33.
[35] Edison TNJI, Atchudan R, Sethuraman MG, Shim JJ, Lee YR. Microwave assisted green synthesis of fluorescent N-doped carbon dots: cytotoxicity and bioimaging applications. *Journal of Photochemistry and Photobiology B: Biology.* 2016 Aug 1;161:154–61.
[36] Schneider J, Reckmeier CJ, Xiong Y, von Seckendorff M, Susha AS, Kasák P, et al. Molecular fluorescence in citric acid-based carbon dots. *J Phys Chem C.* 2017 Jan 26;121(3):2014–22.
[37] Wang H, Lu F, Ma C, Ma Y, Zhang M, Wang B, et al. Carbon dots with positive surface charge from tartaric acid and m-aminophenol for selective killing of Gram-positive bacteria. *Journal of Materials Chemistry B.* 2021;9(1):125–30.
[38] Sahiner N, Suner SS, Sahiner M, Silan C. Nitrogen and sulfur doped carbon dots from amino acids for potential biomedical applications. *J Fluoresc.* 2019 Sep 1;29(5):1191–200.

[39] Li L, Zhang R, Lu C, Sun J, Wang L, Qu B, et al. In situ synthesis of NIR-light emitting carbon dots derived from spinach for bio-imaging applications. *J Mater Chem B.* 2017 Sep 13;5(35):7328–34.

[40] Bandi R, Reddy Gangapuram B, Dadigala R, Eslavath R, S. Singh S, Guttena V. Facile and green synthesis of fluorescent carbon dots from onion waste and their potential applications as sensor and multicolour imaging agents. *RSC Advances.* 2016;6(34): 28633–9.

[41] Mehta VN, Jha S, Basu H, Singhal RK, Kailasa SK. One-step hydrothermal approach to fabricate carbon dots from apple juice for imaging of mycobacterium and fungal cells. *Sensors and Actuators B: Chemical.* 2015 Jul 5;213:434–43.

[42] Prasannan A, Imae T. One-pot synthesis of fluorescent carbon dots from orange waste peels. *Ind Eng Chem Res.* 2013 Nov 6;52(44):15673–8.

[43] Phadke C, Mewada A, Dharmatti R, Thakur M, Pandey S, Sharon M. Biogenic synthesis of fluorescent carbon dots at ambient temperature using Azadirachta indica (Neem) gum. *J Fluoresc.* 2015 Jul 1;25(4):1103–7.

[44] Wang X, Zhang Y, Kong H, Cheng J, Zhang M, Sun Z, et al. Novel mulberry silkworm cocoon-derived carbon dots and their anti-inflammatory properties. *Artificial Cells, Nanomedicine, and Biotechnology.* 2020 Jan 1;48(1):68–76.

[45] Jiang C, Wu H, Song X, Ma X, Wang J, Tan M. Presence of photoluminescent carbon dots in Nescafe§original instant coffee: applications to bioimaging. *Talanta.* 2014 Sep 1;127:68–74.

[46] Hu Y, Yang J, Tian J, Jia L, Yu JS. Waste frying oil as a precursor for one-step synthesis of sulfur-doped carbon dots with pH-sensitive photoluminescence. *Carbon.* 2014 Oct 1;77:775–82.

[47] Wang D, Zhu L, Mccleese C, Burda C, Chen JF, Dai L. Fluorescent carbon dots from milk by microwave cooking. *RSC Advances.* 2016;6(47):41516–21.

[48] Zhang Z, Sun W, Wu P. Highly photoluminescent carbon dots derived from egg white: facile and green synthesis, photoluminescence properties, and multiple applications. *ACS Sustainable Chem Eng.* 2015 Jul 6;3(7):1412–8.

[49] Yang X, Zhuo Y, Zhu S, Luo Y, Feng Y, Dou Y. Novel and green synthesis of high-fluorescent carbon dots originated from honey for sensing and imaging. *Biosensors and Bioelectronics.* 2014 Oct 15;60:292–8.

[50] Zhang M, Wang H, Liu P, Song Y, Huang H, Shao M, et al. Biotoxicity of degradable carbon dots towards microalgae Chlorella vulgaris. *Environ Sci: Nano.* 2019 Nov 7;6(11):3316–23.

[51] Godavarthi S, Mohan Kumar K, Vázquez Vélez E, Hernandez-Eligio A, Mahendhiran M, Hernandez-Como N, et al. Nitrogen doped carbon dots derived from Sargassum fluitans as fluorophore for DNA detection. *Journal of Photochemistry and Photobiology B: Biology.* 2017 Jul 1;172:36–41.

[52] Ramanan V, Thiyagarajan SK, Raji K, Suresh R, Sekar R, Ramamurthy P. Outright green synthesis of fluorescent carbon dots from eutrophic algal blooms for in vitro imaging. *ACS Sustainable Chem Eng.* 2016 Sep 6;4(9):4724–31.

[53] Zhang C, Xiao Y, Ma Y, Li B, Liu Z, Lu C, et al. Algae biomass as a precursor for synthesis of nitrogen-and sulfur-co-doped carbon dots: a better probe in Arabidopsis guard cells and root tissues. *Journal of Photochemistry and Photobiology B: Biology.* 2017 Sep 1;174:315–22.

[54] Agnol LD, Neves RM, Maraschin M, Moura S, Ornaghi HL, Dias FTG, et al. Green synthesis of Spirulina-based carbon dots for stimulating agricultural plant growth. *Sustainable Materials and Technologies.* 2021 Dec 1;30:e00347.

[55] Li Y, Liu F, Cai J, Huang X, Lin L, Lin Y, et al. Nitrogen and sulfur co-doped carbon dots synthesis via one-step hydrothermal carbonization of green alga and their multifunctional applications. *Microchemical Journal.* 2019 Jun 1;147:1038–47.

[56] Funke A, Ziegler F. Hydrothermal carbonization of biomass: a summary and discussion of chemical mechanisms for process engineering. *Biofuels, Bioproducts and Biorefining.* 2010;4(2):160–77.

[57] Wang B, Yu J, Sui L, Zhu S, Tang Z, Yang B, et al. Rational design of multi-color-emissive carbon dots in a single reaction system by hydrothermal. *Advanced Science.* 2021;8(1):2001453.

[58] Zhang Y, Wang Y, Feng X, Zhang F, Yang Y, Liu X. Effect of reaction temperature on structure and fluorescence properties of nitrogen-doped carbon dots. *Applied Surface Science.* 2016 Nov 30;387:1236–46.

[59] Medeiros TV de, Manioudakis J, Noun F, Macairan JR, Victoria F, Naccache R. Microwave-assisted synthesis of carbon dots and their applications. *J Mater Chem C.* 2019 Jun 20;7(24):7175–95.

[60] Ang WL, Boon Mee CAL, Sambudi NS, Mohammad AW, Leo CP, Mahmoudi E, et al. Microwave-assisted conversion of palm kernel shell biomass waste to photoluminescent carbon dots. *Sci Rep.* 2020 Dec 3;10(1):21199.

[61] Simsek S, Ozge Alas M, Ozbek B, Genc R. Evaluation of the physical properties of fluorescent carbon nanodots synthesized using Nerium oleander extracts by microwave-assisted synthesis methods. *Journal of Materials Research and Technology.* 2019 May 1;8(3):2721–31.

[62] Dang H, Huang LK, Zhang Y, Wang CF, Chen S. Large-scale ultrasonic fabrication of white fluorescent carbon dots. *Ind Eng Chem Res.* 2016 May 11;55(18):5335–41.

[63] Zhang Y, Xiao J, Zhuo P, Yin H, Fan Y, Liu X, et al. Carbon dots exhibiting concentration-dependent full-visible-spectrum emission for light-emitting diode applications. *ACS Appl Mater Interfaces.* 2019 Dec 11;11(49):46054–61.

[64] Li D, Ushakova EV, Rogach AL, Qu S. Optical properties of carbon dots in the deep-red to near-infrared region are attractive for biomedical applications. *Small.* 2021;17(43):2102325.

[65] Jiang L, Ding H, Xu M, Hu X, Li S, Zhang M, et al. UV–Vis–NIR full-range responsive carbon dots with large multiphoton absorption cross sections and deep-red fluorescence at nucleoli and in vivo. *Small.* 2020;16(19):2000680.

[66] Ding H, Zhou X, Qin B, Zhou Z, Zhao Y. Highly fluorescent near-infrared emitting carbon dots derived from lemon juice and its bioimaging application. *Journal of Luminescence.* 2019 Jul 1;211:298–304.

[67] Tang C, Long R, Tong X, Guo Y, Tong C, Shi S. Dual-emission biomass carbon dots for near-infrared ratiometric fluorescence determination and imaging of ascorbic acid. *Microchemical Journal.* 2021 May 1;164:106000.

[68] Ding H, Ji Y, Wei JS, Gao QY, Zhou ZY, Xiong HM. Facile synthesis of red-emitting carbon dots from pulp-free lemon juice for bioimaging. *J Mater Chem B.* 2017 Jul 4;5(26):5272–7.

[69] Vijeata A, Chaudhary GR, Umar A, Chaudhary S. Distinctive solvatochromic response of fluorescent carbon dots derived from different components of Aegle Marmelos plant. *Engineered Science.* 2021;15:197–209.

[70] Vasimalai N, Vilas-Boas V, Gallo J, de Fátima Cerqueira M, Menéndez-Miranda M, Costa-Fernández JM, et al. Green synthesis of fluorescent carbon dots from spices for in vitro imaging and tumour cell growth inhibition. *Beilstein journal of nanotechnology.* 2018;9(1):530–44.

[71] Gedda G, Sankaranarayanan SA, Putta CL, Gudimella KK, Rengan AK, Girma WM. Green synthesis of multi-functional carbon dots from medicinal plant leaves for antimicrobial, antioxidant, and bioimaging applications. *Sci Rep.* 2023 Apr 19;13(1):6371.

[72] Zhou Y, Zahran EM, Quiroga BA, Perez J, Mintz KJ, Peng Z, et al. Size-dependent photocatalytic activity of carbon dots with surface-state determined photoluminescence. *Applied Catalysis B: Environmental.* 2019 Jul 5;248:157–66.

[73] Han Z, He L, Pan S, Liu H, Hu X. Hydrothermal synthesis of carbon dots and their application for detection of chlorogenic acid. *Luminescence.* 2020;35(7):989–97.

[74] Li J, Ma S, Xiao X, Zhao D. The one-step preparation of green-emissioned carbon dots through hydrothermal route and its application. *Journal of Nanomaterials.* 2019 Apr 17;2019:e8628354.

[75] Chen BB, Liu ML, Li CM, Huang CZ. Fluorescent carbon dots functionalization. *Advances in Colloid and Interface Science.* 2019 Aug 1;270:165–90.

[76] Watcharamongkol T, Khaopueak P, Seesuea C, Wechakorn K. Green hydrothermal synthesis of multifunctional carbon dots from cassava pulps for metal sensing, antioxidant, and mercury detoxification in plants. *Carbon Resources Conversion.* 2024 Jun 1;7(2):100206.

[77] Sun YP, Zhou B, Lin Y, Wang W, Fernando KAS, Pathak P, et al. Quantum-sized carbon dots for bright and colorful photoluminescence. *J Am Chem Soc.* 2006 Jun 1;128(24):7756–7.

[78] Das A, Kundelev EV, Vedernikova AA, Cherevkov SA, Danilov DV, Koroleva AV, et al. Revealing the nature of optical activity in carbon dots produced from different chiral precursor molecules. *Light Sci Appl.* 2022 Apr 11;11(1):92.

[79] Ru Y, Zhang B, Yong X, Sui L, Yu J, Song H, et al. Full-color circularly polarized luminescence of CsPbX3 nanocrystals triggered by chiral carbon dots. *Advanced Materials.* 2023 Feb 1;35(5):2207265.

[80] Zhang Z, Chen J, Yan X, Liu X, Chen Y, Zhao C, et al. One-step microwave preparation of carbon dots-composited G-quartet hydrogels with controllable chirality and circularly polarized luminescence. *Carbon.* 2023 Jan 25;203:39–46.

[81] Zhang Y, Liu X, Fan Y, Guo X, Zhou L, Lv Y, et al. One-step microwave synthesis of N-doped hydroxyl-functionalized carbon dots with ultra-high fluorescence quantum yields. *Nanoscale.* 2016 Aug 18;8(33):15281–7.

[82] Sarma D, Majumdar B, Sarma TK. Carboxyl-functionalized carbon dots as competent visible light photocatalysts for aerobic oxygenation of alkyl benzenes: role of surface functionality. *ACS Sustainable Chem Eng.* 2018 Dec 3;6(12):16573–85.

[83] Horo H, Saha M, Das H, Mandal B, Kundu LM. Synthesis of highly fluorescent, amine-functionalized carbon dots from biotin-modified chitosan and silk-fibroin blend for target-specific delivery of antitumor agents. *Carbohydrate Polymers.* 2022 Feb 1;277:118862.

[84] Zhao D, Zhang R, Liu X, Li X, Xu M, Huang X, et al. Screening of chitosan derivatives-carbon dots based on antibacterial activity and application in anti-Staphylococcus aureus biofilm. *International Journal of Nanomedicine.* 2022 Mar 4;17:937–52.

[85] Liu Y, Liang F, Sun J, Xu X, Deng C, Sun R, et al. A cellulose nanocrystal-carbon dots@cholestrol fluorescent probe for imaging of plasma membrane with extended time scale. *Sensors and Actuators B: Chemical.* 2024 Apr 15;405:135371.

[86] Havrdova M, Hola K, Skopalik J, Tomankova K, Petr M, Cepe K, et al. Toxicity of carbon dots—Effect of surface functionalization on the cell viability, reactive oxygen species generation and cell cycle. *Carbon.* 2016 Apr 1;99:238–48.

[87] Ma X, Dong Y, Sun H, Chen N. Highly fluorescent carbon dots from peanut shells as potential probes for copper ion: The optimization and analysis of the synthetic process. *Materials Today Chemistry.* 2017 Sep 1;5:1–10.

[88] Lu B, Chen X, Ouyang X, Li Z, Yang X, Khan Z, et al. The roles of novel chitooligosaccharide-peanut oligopeptide carbon dots in improving the flavor quality of Chinese cabbage. *Food Chemistry: X.* 2023 Dec 30;20:100963.

[89] Wee SS, Ng YH, Ng SM. Synthesis of fluorescent carbon dots via simple acid hydrolysis of bovine serum albumin and its potential as sensitive sensing probe for lead (II) ions. *Talanta.* 2013 Nov 15;116:71–6.

[90] Konwar A, Gogoi N, Majumdar G, Chowdhury D. Green chitosan–carbon dots nanocomposite hydrogel film with superior properties. *Carbohydrate Polymers.* 2015 Jan 22;115:238–45.

[91] Han B, Wang W, Wu H, Fang F, Wang N, Zhang X, et al. Polyethyleneimine modified fluorescent carbon dots and their application in cell labeling. *Colloids and Surfaces B: Biointerfaces.* 2012 Dec 1;100:209–14.

[92] Gonçalves H, Esteves da Silva JCG. Fluorescent carbon dots capped with peg200 and mercaptosuccinic acid. *J Fluoresc.* 2010 Sep 1;20(5):1023–8.

[93] Zhao X, Zhang J, Shi L, Xian M, Dong C, Shuang S. Folic acid-conjugated carbon dots as green fluorescent probes based on cellular targeting imaging for recognizing cancer cells. *RSC Advances.* 2017;7(67):42159–67.

[94] Wang HJ, Zhang J, Liu YH, Luo TY, He X, Yu XQ. Hyaluronic acid-based carbon dots for efficient gene delivery and cell imaging. *RSC Advances.* 2017;7(25):15613–24.

[95] Wang Z, Yang B, Chen Z, Liu D, Jing L, Gao C, et al. Bioinspired cryoprotectants of glucose-based carbon dots. *ACS Appl Bio Mater.* 2020 Jun 15;3(6):3785–91.

[96] Li D, Fan Y, Shen M, Bányai I, Shi X. Design of dual drug-loaded dendrimer/carbon dot nanohybrids for fluorescence imaging and enhanced chemotherapy of cancer cells. *J Mater Chem B.* 2019 Jan 2;7(2):277–85.

[97] Zulfajri M, Sudewi S, Damayanti R, Gary Huang G. Rambutan seed waste-derived nitrogen-doped carbon dots with l -aspartic acid for the sensing of Congo red dye. *RSC Advances.* 2023;13(10):6422–32.

[98] Li Z, Wang T, Gu L, Wang H, Zhao Y, Lu S, et al. N-doped carbon dots modified with the epithelial cell adhesion molecule antibody as an imaging agent for HepG2 cells using their ultra-sensitive response to Al3+. *Nanotechnology.* 2020 Oct;31(48):485703.

[99] Demir B, Moulahoum H, Ghorbanizamani F, Barlas FB, Yesiltepe O, Gumus ZP, et al. Carbon dots and curcumin-loaded CD44-Targeted liposomes for imaging and tracking cancer chemotherapy: A multi-purpose tool for theranostics. *Journal of Drug Delivery Science and Technology.* 2021 Apr 1;62: 102363.

[100] Li Z, Ni J, Liu L, Gu L, Wu Z, Li T, et al. Imaging-guided chemo–photothermal polydopamine carbon dots for EpCAM-targeted delivery toward liver tumor. *ACS Appl Mater Interfaces.* 2021 Jun 30;13(25):29340–8.

[101] Zhu L, Xu G, Song Q, Tang T, Wang X, Wei F, et al. Highly sensitive determination of dopamine by a turn-on fluorescent biosensor based on aptamer labeled carbon dots and nano-graphite. *Sensors and Actuators B: Chemical.* 2016 Aug 1;231:506–12.

[102] Liu R, Zhang L, Zhao J, Luo Z, Huang Y, Zhao S. Aptamer and IR820 dual-functionalized carbon dots for targeted cancer therapy against hypoxic tumors based on an 808 nm laser-triggered three-pathway strategy. *Advanced Therapeutics.* 2018;1(5):1800041.

[103] Rai S, Singh BK, Bhartiya P, Singh A, Kumar H, Dutta PK, et al. Lignin derived reduced fluorescence carbon dots with theranostic approaches: Nano-drug-carrier and bioimaging. *Journal of Luminescence.* 2017 Oct 1;190:492–503.

[104] Zhang L, Wang Z, Wang H, Dong W, Liu Y, Hu Q, et al. Nitrogen-doped carbon dots for wash-free imaging of nucleolus orientation. *Microchim Acta.* 2021 May 10;188(6):183.

[105] Sachdev A, Matai I, Gopinath P. Dual-functional carbon dots–silver@zinc oxide nanocomposite: in vitro evaluation of cellular uptake and induction of apoptosis. *J Mater Chem B.* 2015 Feb 4;3(7):1217–29.

[106] Guan C, Zhao Y, Hou Y, Shan G, Yan D, Liu Y. Glycosylated liposomes loading carbon dots for targeted recognition to HepG2 cells. *Talanta.* 2018 May 15;182:314–23.

[107] Mohammadi S, Salimi A, Hoseinkhani Z, Ghasemi F, Mansouri K. Carbon dots hybrid for dual fluorescent detection of microRNA-21 integrated bioimaging of MCF-7 using a microfluidic platform. *Journal of Nanobiotechnology.* 2022 Feb 8;20(1):73.

[108] Shen Y, Wu T, Wang Y, Zhang SL, Zhao X, Chen HY, et al. Nucleolin-targeted ratiometric fluorescent carbon dots with a remarkably large emission wavelength shift for precise imaging of cathepsin B in living cancer cells. *Anal Chem.* 2021 Mar 2;93(8):4042–50.

[109] Shu M, Gao F, Yu C, Zeng M, He G, Wu Y, et al. Dual-targeted therapy in HER2-positive breast cancer cells with the combination of carbon dots/HER3 siRNA and trastuzumab. *Nanotechnology.* 2020 May;31(33):335102.

[110] Zhang X, Chen L, Wei YY, Yang YZ, Liu XG, Du JL, et al. Advances in organelle-targeting carbon dots. *Fullerenes, Nanotubes and Carbon Nanostructures.* 2021 May 4;29(5):394–406.

[111] Jung YK, Shin E, Kim BS. Cell nucleus-targeting zwitterionic carbon dots. *Sci Rep.* 2015 Dec 22;5(1):18807.

[112] He H, Chen X, Feng Z, Liu L, Wang Q, Bi S. Nanoscopic imaging of nucleolar stress enabled by protein-mimicking carbon dots. *Nano Lett.* 2021 Jul 14;21(13):5689–96.

[113] Hua XW, Bao YW, Wu FG. Fluorescent carbon quantum dots with intrinsic nucleolus-targeting capability for nucleolus imaging and enhanced cytosolic and

nuclear drug delivery. *ACS Appl Mater Interfaces.* 2018 Apr 4;10(13):10664–77.

[114] Geng X, Sun Y, Li Z, Yang R, Zhao Y, Guo Y, et al. Retrosynthesis of tunable fluorescent carbon dots for precise long-term mitochondrial tracking. *Small.* 2019;15(48):1901517.

[115] Guo S, Sun Y, Li J, Geng X, Yang R, Zhang X, et al. Fluorescent carbon dots shuttling between mitochondria and the nucleolus for in situ visualization of cell viability. *ACS Appl Bio Mater.* 2021 Jan 18;4(1):928–34.

[116] Geng X, Sun Y, Guo Y, Zhao Y, Zhang K, Xiao L, et al. Fluorescent carbon dots for in situ monitoring of lysosomal ATP levels. *Anal Chem.* 2020 Jun 2;92(11):7940–6.

[117] Chen H, Wang GD, Tang W, Todd T, Zhen Z, Tsang C, et al. Gd-encapsulated carbonaceous dots with efficient renal clearance for magnetic resonance imaging. *Advanced materials (Deerfield Beach, Fla).* 2014;26(39):6761.

[118] Liao J, Yao Y, Lee CH, Wu Y, Li P. In vivo biodistribution, clearance, and biocompatibility of multiple carbon dots containing nanoparticles for biomedical application. *Pharmaceutics.* 2021 Nov;13(11):1872.

[119] Srivastava I, Sar D, Mukherjee P, Schwartz-Duval AS, Huang Z, Jaramillo C, et al. Enzyme-catalysed biodegradation of carbon dots follows sequential oxidation in a time dependent manner. *Nanoscale.* 2019 Apr 25;11(17):8226–36.

[120] Yang Y, Ren X, Sun Z, Fu C, Liu T, Meng X, et al. Toxicity and bio-distribution of carbon dots after single inhalation exposure in vivo. *Chinese Chemical Letters.* 2018 Jun 1;29(6):895–8.

[121] Huang X, Zhang F, Zhu L, Choi KY, Guo N, Guo J, et al. Effect of injection routes on the biodistribution, clearance, and tumor uptake of carbon dots. *ACS Nano.* 2013 Jul 23;7(7):5684–93.

[122] Liu Z, Chen W, Li Y, Xu Q. Integrin $\alpha v\beta 3$-targeted C-dot nanocomposites as multifunctional agents for cell targeting and photoacoustic imaging of superficial malignant tumors. *Anal Chem.* 2016 Dec 6;88(23):11955–62.

[123] Bhunia SK, Maity AR, Nandi S, Stepensky D, Jelinek R. Imaging cancer cells expressing the folate receptor with carbon dots produced from folic acid. *ChemBioChem.* 2016;17(7):614–9.

[124] Seven E, Seven YB, Zhou Y, Poudel-Sharma S, Diaz-Rucco JJ, Cilingir EK, et al. Crossing the blood–brain barrier with carbon dots: uptake mechanism and in vivo cargo delivery. *Nanoscale Advances.* 2021;3(13):3942–53.

[125] Yuan Y, Guo B, Hao L, Liu N, Lin Y, Guo W, et al. Doxorubicin-loaded environmentally friendly carbon dots as a novel drug delivery system for nucleus targeted cancer therapy. *Colloids and Surfaces B: Biointerfaces.* 2017 Nov 1;159:349–59.

[126] Chowdhury M, Kumar Das P. Paclitaxel-loaded biotinylated Fe2+-doped carbon dot: combination therapy in cancer treatment. *ACS Appl Bio Mater.* 2021 Jun 21;4(6):5132–44.

[127] Ahmed A, Shahadat M, Shahid ul Islam, Adnan R, Mohamad Ibrahim MN, Ullah Q. Synthesis, characterization, and properties of green carbon nanodots. In: *Green Carbon Materials for Environmental Analysis: Emerging Research and Future Opportunities*. American Chemical Society; 2023. p. 25–39. (ACS Symposium Series; vol. 1441). Available from: https://doi.org/10.1021/bk-2023-1441.ch002

[128] Campalani C, Rigo D. Continuous flow synthesis and applications of carbon dots: a mini-review. *Next Sustainability*. 2023 Mar 1;1:100001.

[129] Gellé A, Jin T, de la Garza L, Price GD, Besteiro LV, Moores A. Applications of plasmon-enhanced nanocatalysis to organic transformations. *Chem Rev*. 2020 Jan 22;120(2):986–1041.

[130] Chong Y, Ma Y, Shen H, Tu X, Zhou X, Xu J, et al. The in vitro and in vivo toxicity of graphene quantum dots. *Biomaterials*. 2014 Jun 1;35(19):5041–8.

[131] Wang Y, Guo G, Gao J, Li Z, Yin X, Zhu C, et al. Multicenter-emitting carbon dots: color tunable fluorescence and dynamics monitoring oxidative stress in vivo. *Chem Mater*. 2020 Oct 13;32(19):8146–57.

[132] Zhang W, Sigdel G, Mintz KJ, Seven ES, Zhou Y, Wang C, et al. Carbon dots: a future blood–brain barrier penetrating nanomedicine and drug nanocarrier. *International Journal of Nanomedicine*. 2021 Jul 23 [cited 2024 Mar 27]; Available from: https://www.tandfonline.com/doi/abs/10.2147/IJN.S318732

[133] Luo P, Li C, Shi G. Synthesis of gold@ carbon dots composite nanoparticles for surface enhanced Raman scattering. *Physical Chemistry Chemical Physics*. 2012;14(20):7360–6.

[134] Ge J, Jia Q, Liu W, Guo L, Liu Q, Lan M, et al. Red-emissive carbon dots for fluorescent, photoacoustic, and thermal theranostics in living mice. *Advanced Materials*. 2015;28(27):4169–77.

[135] Choi G, Rejinold NS, Piao H, Choy JH. Inorganic–inorganic nanohybrids for drug delivery, imaging and photo-therapy: recent developments and future scope. *Chemical Science*. 2021;12(14):5044–63.

[136] Kaur H, Sareen S, Mutreja V, Verma M. Spinach-derived carbon dots for the turn-on detection of chromium ions (Cr3+). *J Inorg Organomet Polym*. 2023 Dec 1;33(12):3703–15.

[137] Ren G, Tang M, Chai F, Wu H. One-pot synthesis of highly fluorescent carbon dots from spinach and multipurpose applications. *European Journal of Inorganic Chemistry*. 2018;2018(2):153–8.

[138] Won S, Kim JS. Spinach extract derived carbon dots decorated on ZnO nanorods for photocatalytic dye degradation. *Science of Advanced Materials*. 2021 May 1;13(5):922–6.

[139] Xu X, Cai L, Hu G, Mo L, Zheng Y, Hu C, et al. Red-emissive carbon dots from spinach: Characterization and application in visual detection of time. *Journal of Luminescence*. 2020 Nov 1;227:117534.

[140] Yao Z, Lai Z, Chen C, Xiao S, Yang P. Full-color emissive carbon-dots targeting cell walls of onion for in situ imaging of heavy metal pollution. *Analyst*. 2019 May 28;144(11):3685–90.

[141] Ventrella A, Camisasca A, Fontana A, Giordani S. Synthesis of green fluorescent carbon dots from carbon nano-onions and graphene oxide. *RSC Advances*. 2020;10(60):36404–12.

[142] Hu Y, Zhang L, Li X, Liu R, Lin L, Zhao S. Green preparation of S and N Co-Doped carbon dots from water chestnut and onion as well as their use as an off–on fluorescent probe for the quantification and imaging of coenzyme A. *ACS Sustainable Chem Eng*. 2017 Jun 5;5(6):4992–5000.

[143] Salimi Shahraki H, Qurtulen, Ahmad A. Synthesis, characterization of carbon dots from onion peel and their application as absorbent and anticancer activity. *Inorganic Chemistry Communications*. 2023 Apr 1;150:110514.

[144] Aggarwal R, Saini D, Singh B, Kaushik J, Garg AK, Sonkar SK. Bitter apple peel derived photoactive carbon dots for the sunlight induced photocatalytic degradation of crystal violet dye. *Solar Energy*. 2020 Feb 1;197:326–31.

[145] Chatzimarkou A, Chatzimitakos TG, Kasouni A, Sygellou L, Avgeropoulos A, Stalikas CD. Selective FRET-based sensing of 4-nitrophenol and cell imaging capitalizing on the fluorescent properties of carbon nanodots from apple seeds. *Sensors and Actuators B: Chemical*. 2018 Apr 1;258:1152–60.

[146] Li Z, Zhang Y, Niu Q, Mou M, Wu Y, Liu X, et al. A fluorescence probe based on the nitrogen-doped carbon dots prepared from orange juice for detecting Hg2+ in water. *Journal of Luminescence*. 2017 Jul 1;187:274–80.

[147] Kumar D, Singh K, Verma V, Bhatti HS. Synthesis and characterization of carbon quantum dots from orange juice. *Journal of Bionanoscience*. 2014 Aug 1;8(4):274–9.

[148] Mewada A, Pandey S, Shinde S, Mishra N, Oza G, Thakur M, et al. Green synthesis of biocompatible carbon dots using aqueous extract of Trapa bispinosa peel. *Materials Science and Engineering: C*. 2013 Jul 1;33(5):2914–7.

[149] Raina S, Thakur A, Sharma A, Pooja D, Minhas AP. Bactericidal activity of Cannabis sativa phytochemicals from leaf extract and their derived Carbon Dots and Ag@Carbon Dots. *Materials Letters*. 2020 Mar 1;262:127122.

[150] Vijeata A, Chaudhary GR, Chaudhary S, Umar A. Biogenic synthesis of highly fluorescent carbon dots using Azadirachta indica leaves: An eco-friendly approach with enhanced photocatalytic degradation efficiency towards Malachite green. *Chemosphere*. 2023 Nov 1;341:139946.

[151] Feng J, Wang WJ, Hai X, Yu YL, Wang JH. Green preparation of nitrogen-doped carbon dots derived from silkworm chrysalis for cell imaging. *J Mater Chem B*. 2016 Jan 6;4(3):387–93.

[152] Crista DMA, El Mragui A, Algarra M, Esteves da Silva JCG, Luque R, Pinto da Silva L. Turning spent coffee grounds into sustainable precursors for the fabrication of carbon dots. *Nanomaterials*. 2020 Jun;10(6):1209.

[153] Zhang W, Jia L, Guo X, Yang R, Zhang Y, Zhao Z. Green synthesis of up- and down-conversion photoluminescent carbon dots from coffee beans for Fe3+ detection and cell imaging. *Analyst*. 2019 Dec 2;144(24):7421–31.

[154] Hong WT, Yang HK. Anti-counterfeiting application of fluorescent carbon dots derived from wasted coffee grounds. *Optik*. 2021 Sep 1;241:166449.

[155] K K, V BM, P N. A green approach for synthesis of highly fluorescent carbon dots from waste engine oil: A strategy for waste to value added products. *Diamond and Related Materials*. 2022 Jan 1;121:108724.

[156] Murru C, Badía-Laíño R, Díaz-García ME. Synthesis and characterization of green carbon dots for scavenging radical oxygen species in aqueous and oil samples. *Antioxidants*. 2020 Nov;9(11):1147.

[157] Han S, Zhang H, Xie Y, Liu L, Shan C, Li X, et al. Application of cow milk-derived carbon dots/Ag NPs composite as the antibacterial agent. *Applied Surface Science*. 2015 Feb 15;328:368–73.

[158] Kumar A, Kumar I, Gathania AK. Synthesis, characterization and potential sensing application of carbon dots synthesized via the hydrothermal treatment of cow milk. *Sci Rep*. 2022 Dec 28;12(1):22495.

[159] Cardoso-Ávila PE, Pichardo-Molina JL, Vázquez-Olmos M, González-Aguiñaga E. Chicken egg white as a "greener" biomass source for the rapid synthesis of fluorescent carbon dots. *Materials Letters*. 2024 Mar 1;358:135880.

[160] Yu L, He M, Liu S, Dou X, Li L, Gu N, et al. Fluorescent egg white-based carbon dots as a high-sensitivity iron chelator for the therapy of nonalcoholic fatty liver disease by iron overload in zebrafish. *ACS Appl Mater Interfaces*. 2021 Nov 24;13(46):54677–89.

[161] Mandani S, Dey D, Sharma B, Sarma TK. Natural occurrence of fluorescent carbon dots in honey. *Carbon*. 2017 Aug 1;119:569–72.

[162] Surendran P, Lakshmanan A, Priya SS, Balakrishnan K, Rameshkumar P, Kannan K, et al. Bioinspired fluorescence carbon quantum dots extracted from natural honey: Efficient material for photonic and antibacterial applications. *Nano-Structures & Nano-Objects*. 2020 Oct 1;24:100589.

[163] Wu S, Li W, Zhou W, Zhan Y, Hu C, Zhuang J, et al. Large-scale one-step synthesis of carbon dots from yeast extract powder and construction of carbon dots/pva fluorescent shape memory material. *Advanced Optical Materials*. 2018;6(7):1701150.

Received 2024-03-03
Accepted 2024-04-14